

GEOCHEMISTRY AND PETROLOGY OF FELDSPAR CRYSTALLIZATION IN THE VĚŽNÁ PEGMATITE, CZECHOSLOVAKIA

PETR ČERNÝ

Department of Earth Sciences, University of Manitoba, Winnipeg, Manitoba R3T 2N2

JOSEPH V. SMITH, ROGER A. MASON¹ AND JEREMY S. DELANEY²

Department of the Geophysical Sciences, University of Chicago, Chicago, Illinois 60637, U.S.A.

ABSTRACT

Atomic-absorption spectrophotometry, electron-microprobe and ion-microprobe techniques were used to analyze 33 samples of K-feldspar and 34 of plagioclase from the Věžná pegmatite, Czechoslovakia, to establish the distribution of major (Si, Al, Na, Ca, K) and trace (Li, Rb, Cs, Mg, Sr, Ba, Pb, Fe, Ti, P, F) elements and their fractionation trends in the sequence of feldspar crystallization. The pegmatite consists of an anthophyllite + phlogopite (+ tremolite) reaction zone along contacts with the enclosing serpentinite, coarse-grained plg + K-fsp + qtz wall zone, megacrystic K-fsp + qtz intermediate graphic-textured and blocky zones, and segmented quartz core. Cleavelandite and subordinate saccharoidal albite (the latter associated with minerals of Be, Ti, Nb, Ta, Zr, REE) replace the intermediate zones, and adularia with albite occurs in late fissures. Microperthitic orthoclase predominates over vein perthite with subordinate intermediate microcline; plagioclase compositions covering the peristerite range are homogeneous to X-rays. In the primary sequence, Na, Rb, P, K/Ba, (Li?, Ti?, F?) increase and Ba, Sr, K/Na, K/Rb, Ba/Rb, Ba/Sr, (Cs?) decrease in K-feldspar. Most of these trends become reversed in the late K-feldspar (adularia). Plagioclase shows a prominent gap between the primary oligoclase and late metasomatic albite, but an increase in Na, P, Na/Ca and decrease in Ca, Sr, Ba (Li?, Cs?) are observed throughout the crystallization of plagioclase. Mg, Fe, Ti, Pb, B and F appear to vary erratically. The primary crystallization of the feldspars probably proceeded in the K-feldspar liquidus-solidus loop of the alkali feldspars + quartz + volatiles system, at about 2.5 kbar P(H₂O) and 700 to 600°C, coupled with nonequilibrium precipitation of wall-zone oligoclase due to assimilation of Ca from the host rock. Potassium depletion led to enrichment of Na in the residual subsolidus fluids and subsequent albitic replacements. Adularia and albite precipitated under low P, T conditions.

Keywords: feldspar, pegmatite, geochemistry, petrogenesis, electron microprobe, ion microprobe, trace elements, Věžná, Czechoslovakia.

¹Present address: Bullard Laboratories, Department of Earth Sciences, University of Cambridge, Cambridge, Great Britain CB3 0EZ.

²Present address: Department of Mineral Sciences, American Museum of Natural History, New York, N.Y. 10024, U.S.A.

SOMMAIRE

On a analysé, par spectrophotométrie d'absorption atomique et techniques des microsondes électronique et ionique, 33 échantillons de feldspath potassique et 34 de plagioclase provenant de la pegmatite de Věžná (Tchécoslovaquie), dans le but d'établir la distribution des éléments majeurs (Si, Al, Na, Ca, K) et en traces (Li, Rb, Cs, Mg, Sr, Ba, Pb, Fe, Ti, P, F) et leur comportement pendant la séquence de cristallisation des feldspaths. La pegmatite comporte une zone de réaction à anthophyllite + phlogopite (+ trémolite) le long des contacts avec la serpentinite encaissante, une zone externe à plagioclase, feldspath potassique et quartz à grains grossiers, des zones intermédiaires à mégacristaux de feldspath potassique avec quartz en texture graphique et en blocs, et un noyau de quartz segmenté. Cleavelandite et albite saccharoïde (celle-ci, en faible proportion, associée aux minéraux de Be, Ti, Nb, Ta, Zr, terres rares) remplacent les roches des zones intermédiaires; adulaire et albite occupent les fissures formées tardivement. L'orthose microperthitique domine par rapport à la perthite à texture en veinules, qui contient une microcline intermédiaire subordonnée. Les compositions du plagioclase, dans l'intervalle de la péristérite, sont homogènes aux rayons X. Dans la séquence primaire de cristallisation, Na, Rb, P, K/Ba, Li(?), Ti(?) et F(?) augmentent tandis que Ba, Sr, K/Na, K/Rb, Ba/Rb, Ba/Sr et Cs(?) diminuent dans le feldspath potassique. La plupart de ces caractéristiques sont inversées dans l'adulaire tardive. Une grande lacune sépare l'oligoclase primaire de l'albite métasomatique tardive, quoiqu'en général, Na, P et Na/Ca augmentent tandis que Ca, Sr, Ba, Li(?) et Cs(?) diminuent au cours de la cristallisation du plagioclase. Mg, Fe, Ti, Pb, B et F semblent varier de façon aléatoire. La cristallisation primaire des feldspaths aurait été régie par la courbe liquidus-solidus dans le système feldspaths alcalins + quartz + phase gazeuse, à environ 2.5 kbar de pression d'eau et de 700 à 600°C; on attribue à l'assimilation du calcium des roches encaissantes la précipitation en déséquilibre de l'oligoclase dans la zone externe. L'appauvrissement du système en potassium a causé l'enrichissement en Na des fluides résiduels au stade subsolidus, suivi de remplacements albitiques. L'adulaire et l'albite des fissures se sont formées à faibles pression et température.

(Traduit par la Rédaction)

Mots-clés: feldspaths, pegmatite, géochimie, pétrogénèse, microsonde électronique, microsonde ionique, éléments en traces, Věžná, Tchécoslovaquie.

INTRODUCTION

Geochemical studies of feldspars in granitic pegmatites have been concerned mainly with regional variations and petrogenetic implications (Heier & Taylor 1959, Shimanskii & Uchakin 1962, Manuylova *et al.* 1966, Lappalainen & Neuvonen 1968, Neiva 1977, Černý *et al.* 1981), with utilization of feldspars as indicators for geochemical exploration (Gordiyenko 1964, 1971, 1976, Shmakin 1979, Černý *et al.* 1981), with local equilibria and conditions of crystallization (Kretz 1970, Martin 1974), with low-temperature reconstitution (Stretenskaya 1963, Bachinski & Orville 1969, Fisher 1971, Černý & Macek 1972) and with other restricted features and assemblages (Taylor *et al.* 1960, Taylor *et al.* 1979, Foord & Martin 1979). Papers covering broader aspects of feldspar crystallization within a given pegmatite are scarce (Carl 1962, Correia Neves 1964, Tan 1966, Schwarzer 1969, Foord 1976, Černý & Macek 1974), even though the feldspars are potential indicators for most of the crystallization history (Martin 1982).

Existing chemical data obtained by X-ray-fluorescence spectrometry, atomic-absorption spectrophotometry and optical-emission spectrography may be affected by impurities in the relatively large samples of feldspars. Inclusions or late trains of albite in K-feldspar, relics of K-feldspar in metasomatic albite, alteration to mica or clay and turbidity may be unavoidable in sample preparation. Impurities generate either general scatter or systematic shifts of data that may lead to erroneous interpretations, as pointed out by Černý & Macek (1972, 1974).

In order to bypass this problem, JVS set up a collaborative program in 1978 to evaluate the potential of electron and ion microprobes for the determination of feldspar chemistry in relation to crystallization sequences in pegmatites. Several pegmatites were selected to cover a range of internal complexity, geochemical classes and paragenetic types. This paper presents the results obtained for a pegmatite from Věžná, Czechoslovakia, which carries minerals of Be, B, Ti, Nb, Ta, Zr and REE and which is poor in Li, Rb, and Cs (Černý 1965, 1968a, 1971, Černý *et al.* 1964, Černý & Miškovský 1966, Černý & Povondra 1966). Although the electron and ion microprobes provided analyses mostly unaffected by mechanical impurities, there are new problems that restrict the value of the analytical data. Firstly, most of the Věžná feldspars are turbid, and only small areas are suitable for microprobe analysis. Secondly, the K-feldspar typically is micropertitic, and chemically inhomogeneous on the scale of micrometres because of diffusion-controlled disequilibrium (*cf.* Mason 1982). Because the number of analyses (especially with the ion probe) was restricted by time and money, it was not possible to obtain a reliable estimate of the bulk compo-

sition of individual feldspar phases. Nevertheless, the probe data correlate quite well with the paragenetic sequence of pegmatite units, and provide a useful guide to the chemical fractionation of the trace elements.

OCCURRENCE

The pegmatite lies south of the village of Věžná in western Moravia (49°26'50"N, 33°56'26"E) at the northeastern margin of the Moldanubicum, a block of Proterozoic terrane reworked during the Hercynian orogeny of central and western Europe. It is exposed in the western part of a serpentinized harzburgite enclave, one of several tectonic rafts of ultrabasic rocks enclosed in an otherwise monotonous migmatitic gneissic terrane in the amphibolite metamorphic facies.

The pegmatite penetrated a fracture in the enclosing serpentinite; it contains locally angular xenoliths of serpentinite. It is tabular in overall shape, striking NNW and dipping 50 to 80° SSW. It is exposed for about 40 m along strike but probably extends farther, as both extremities are covered by slope talus and soil. The width varies from 1.5 to 2.5 m.

Injection of the pegmatite was evidently very late in the regional geological evolution, postdating the regional metamorphism, tectonic emplacement of the harzburgite raft and its subsequent serpentinization. The pegmatite is not affected by the development of chlorite, saponite, talc-related phases and other minerals that replace feldspars and quartz in pegmatites emplaced prior to serpentinization (Černý 1968b); in contrast, these minerals are extensively developed in the migmatitic gneisses.

INTERNAL STRUCTURE AND PARAGENESIS

The bilateral structure of the pegmatite examined is disturbed only by metasomatic assemblages (Fig. 1a). From margins to centre, the following units are distinguished: reaction zone at the contact with serpentinite, wall zone of granular pegmatite, intermediate graphic zone, intermediate blocky zone, and quartz core.

The footwall part of the wall zone is largely replaced by a plagioclase + phlogopite unit. Albitic replacements, late rare-element mineralization and open-fissure assemblages penetrate the intermediate zones and quartz core but do not obliterate the primary compositional and textural features.

The reaction zone consists of a layer of fibrous anthophyllite (4–6 cm wide, oriented subnormal to the serpentinite wall-rock), a discontinuous scatter of randomly oriented tremolite and a layer of phlogopite (2–5 cm wide, adjacent to the wall zone, with the mica flakes subparallel to the general attitude of the pegmatite contact).

The wall zone consists of a granular assemblage

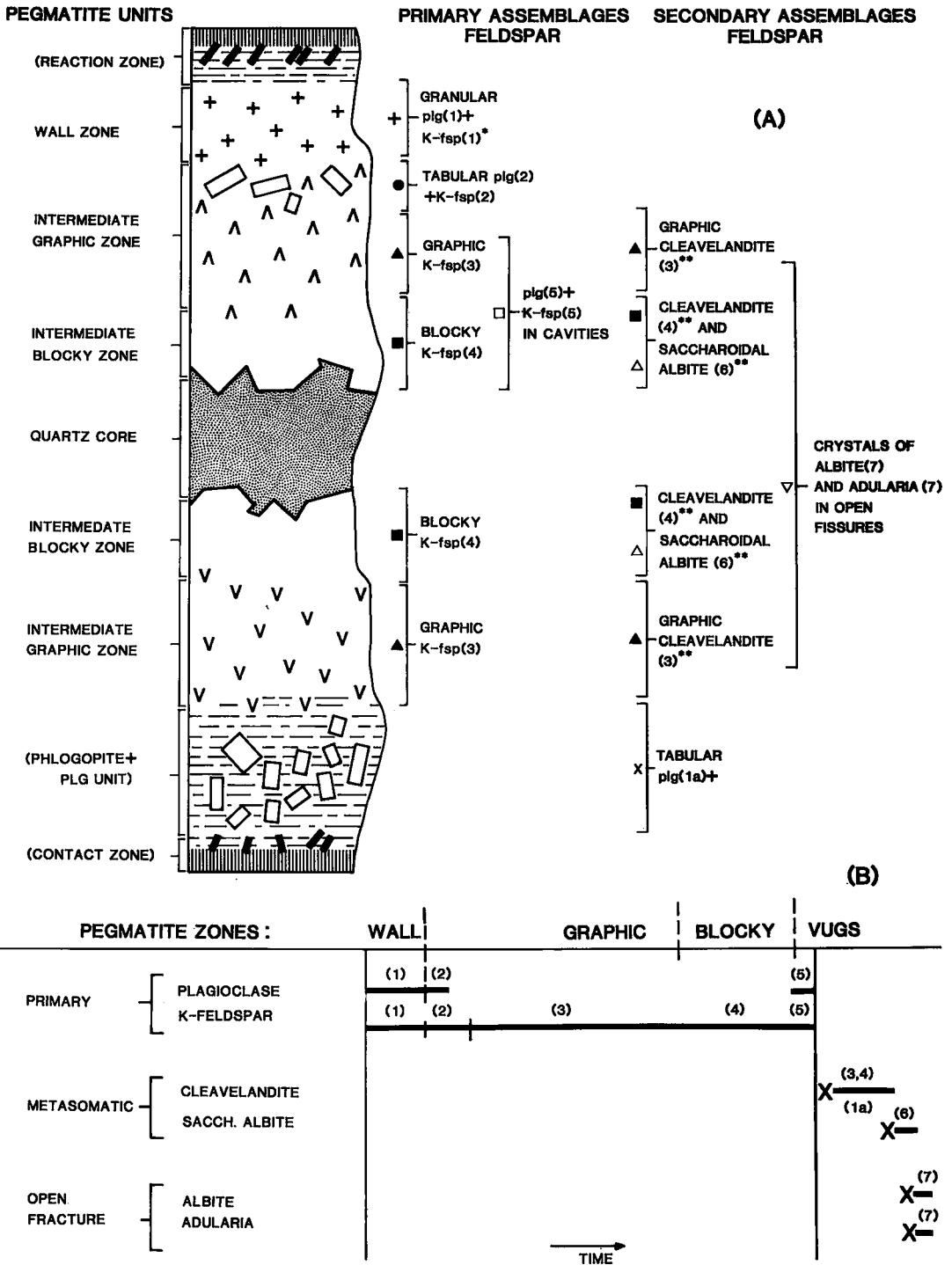


FIG. 1. Zoning, feldspar assemblages and mineral associations of the Věžná pegmatite. (a) Spatial relations: (1) *associated with biotite; (3), (4) **associated with biotite, beryllian cordierite, beryl, tourmaline, niobian rutile, zircon, xenotime, monazite, rarely muscovite, columbite; (1a) + associated with phlogopite, apatite, rarely tourmaline; (7) + + associated with quartz, celadonite, milarite, bavenite, epididymite, eudidymite, rarely microlite, fluorite. (b) Crystallization sequence of the feldspar assemblages: X denotes deformation and fracturing of pre-existing minerals, before the onset of crystallization of the secondary feldspars.

of K-feldspar + plagioclase + quartz, with grain size between 5 and 40 mm. Feldspars are equidimensional, with simple polygonal outlines; quartz is irregular, partly interstitial to the feldspars, and locally quasi-graphic. Modal analyses cluster closely around the average of 40% plagioclase, 27% K-feldspar and 33% quartz. The feldspars of this zone are designated as granular plagioclase (1) and K-feldspar (1) (Fig. 1).

The *intermediate graphic zone*, at its border with the wall zone, contains thick subhedral tabular plagioclase (2) and tabular K-feldspar (2) with sub-graphic quartz (up to 6 cm in size, with interstitial quartz), but it mostly consists of a graphic intergrowth of 71% K-feldspar (3) with 29% quartz. Coarse K-feldspar individuals are as much as 30 cm long. The graphic quartz rods vary from 2 to 35 mm across, and may reach 20 cm in length. The size of the quartz rods increases from centre to margin of K-feldspar individuals, and from outer parts of the

intermediate graphic zone inward. Most quartz rods are single crystals, and mosaic recrystallization is rare. Within any crystal of K-feldspar (3), the orientation of quartz rods is uniform. Flat tabular quartz grains are commonly located along intergranular contacts of K-feldspar grains; their orientations are random, and different from that of graphic quartz inside the flanking feldspar.

The graphic K-feldspar + quartz zone is penetrated by a graphic intergrowth of platy cleavelandite (3) and quartz. In contrast to the classic shape, orientation and distribution of the quartz hosted by K-feldspar (3), the quartz rods in divergent sheafs of curved cleavelandite plates are rather round and irregular, commonly granulated and with diverse orientations (Fig. 2a, b). Margins of cleavelandite (3) + quartz aggregates indicate replacement of both K-feldspar (3) and quartz of the primary intermediate graphic zone (Fig. 2c). Local graphic intergrowths of beryllian cordierite and

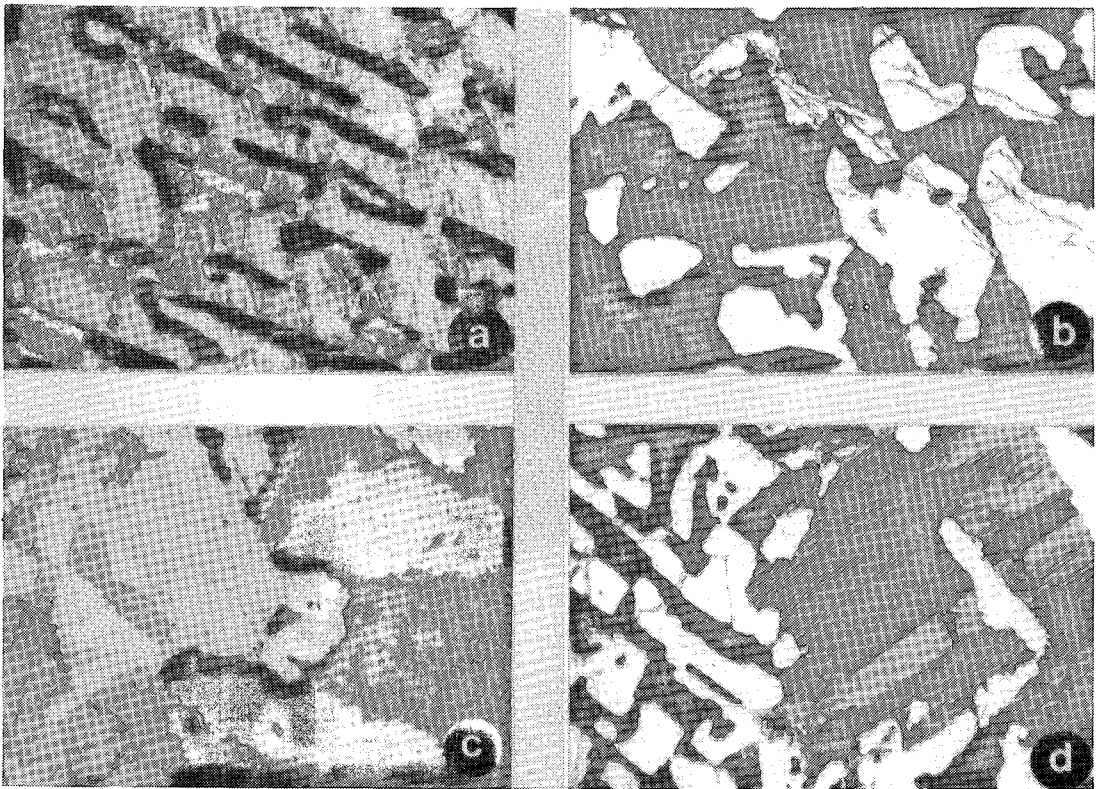


FIG. 2. Textures of feldspar and quartz intergrowths. (a) Graphic intergrowth of quartz (black) and randomly disordered microcline perthite. (b) Graphic intergrowth of quartz (white) and cleavelandite. (c) Quartz rods (black) of K-feldspar and quartz graphic intergrowth (lower right) corroded and recrystallized at contacts with cleavelandite (white) and quartz (pale grey) graphic intergrowth (left). (d) Cleavelandite and quartz (white) graphic intergrowth (right) in contact with cordierite (black) and quartz (white) graphic intergrowth (left). Crossed polars; the width of each photograph is 5 mm.

quartz occur exclusively along this metasomatic contact (Fig. 2d). The average mode of the cleavelandite (3) + quartz intergrowth is 69% cleavelandite and 31% quartz.

The outer margin of the *intermediate blocky zone* is marked by the abrupt disappearance of graphic quartz rods at ghost surfaces within the host feldspar, but otherwise the feldspar crystallization is continuous from the graphic into the blocky zone. The primary blocky zone consists only of blocky K-feldspar (4) crystals up to 40 cm in size. The boundary against the central quartz core is irregular. K-feldspar crystals euhedral against quartz are rare; subhedral blocks of K-feldspar (4) are commonly roughly corrugated in contact with quartz, in a manner resembling interference growth-surfaces of graphic quartz and feldspar.

Platy cleavelandite (4) replaces the blocky K-feldspar (4) along intergranular surfaces and fractures that rarely extend into the quartz core. The platy crystals range between 1 and 6 cm. Quartz is absent in this cleavelandite. In aggregates of cleavelandite crossing the boundary between the graphic and blocky intermediate zones, the graphic quartz is restricted to those parts hosted by graphic K-feldspar + quartz.

Rare and small cavities along the boundary between the graphic and blocky intermediate zones are defined by crystal faces of surrounding K-feldspar crystals and by protruding euhedral terminations of quartz rods where the cavities occur in the graphic zone. Euhedral crystals of plagioclase (5) and K-feldspar (5), up to 7 mm in size, line the vugs along with rare flakes of muscovite.

The position of saccharoidal albite (6) in the paragenetic sequence is somewhat uncertain. Locally, it seems to have gradually developed from the cleavelandite (4). However, most of its restricted occurrences are clearly associated with a Be-, Ti-, Nb-, Ta-, Zr-, REE-bearing assemblage confined to fractures cross-cutting all feldspar types (including cleavelandite) and quartz of both intermediate zones (mostly the blocky one). Thus the saccharoidal albite (6) is treated as an independent generation of plagioclase, postdating cleavelandite (4).

Tabular plagioclase (1a) is the predominant component of the metasomatic unit penetrating along the footwall contact of the pegmatite with serpentinite (Fig. 1). Its subhedral crystals vary between 2 and 15 cm in maximum dimension. The plagioclase is embedded in (and partly intergrown with) phlogopite and apatite; the apatite is particularly abundant along the plagioclase surfaces.

The last generation of feldspars is confined to open fissures populated by products of late hydrothermal activity. Crystals of albite (7) tabular on (010) and of the classic wedge-shaped adularia (7) (both reaching 3 mm in size) are closely associated with

celadonite, secondary beryllium minerals and other phases.

Figure 1(b) summarizes the time sequence for development of the various feldspars in the primary, metasomatic and open-fracture groups.

EXPERIMENTAL METHODS

In view of the narrow and variable width of the pegmatite examined, field sampling of feldspars was aimed at a general representation of each primary zone and metasomatic unit rather than at linear cross-sections. Most samples were collected in the upper half of the bilateral zonal sequence, because of the disturbance of the footwall segment by albitization (1a) along its contact with serpentinite (Fig. 1). However, random sampling of the footwall segments of the intermediate zones shows no deviation from the compositional trends of the hanging-wall segment, and the analyzed samples are representative of the whole pegmatite.

Feldspars were separated manually for chemical analysis, from crushed material (2–4 mm) under a binocular microscope. Bulk compositions of feldspar intergrown with graphic quartz were obtained on samples 5–7 cm in size, crushed and checked for impurities before pulverization. Analyses of the K-feldspar (3) – quartz intergrowths appear to be reliable, but the cleavelandite (3) + quartz aggregates proved to be contaminated by relics of K-feldspar (*cf.* Discussion). Feldspars (1) from the wall zone and adularia (7) are milky to turbid, but the other types of feldspar much less so.

Partial chemical analyses of bulk feldspars and feldspar + quartz intergrowths were performed by flame atomic-absorption spectrophotometry, using 0.5 to 1 g samples. USGS and NBS feldspars and micas were used as standards.

Plagioclase and K-rich areas of K-feldspar were analyzed with electron and ion microprobes. Cleavage fragments were mounted in epoxy cement on silica glass slides and polished to thin-section thickness. Areas free from alteration were selected and photographed prior to the application of a carbon coat. Wavelength-dispersion electron-microprobe analyses were made under the following conditions: accelerating voltage 25 kV, beam current 2.0 μ A, beam diameter 20 μ m (J.S. Delaney, analyst). Feldspar standards for ion-probe analysis were mounted as above and analyzed for minor elements by wavelength-dispersion methods (25 kV, 0.4 μ A, 20 μ m) and for major elements by energy-dispersion methods (15 kV, 0.1 μ A, 20 μ m) (R.A. Mason, analyst). Detection levels for minor elements are between 50 and 100 ppm (2 σ). Major elements are accurate to ~2% of the amount present.

Following electron-probe analysis, the samples and standards were cleaned, coated with gold and loaded

into the ion microprobe. Analytical techniques are described and justified in Steele *et al.* (1980, 1981), Mason (1982) and Mason *et al.* (1982); further calibrations are being prepared for publication. The following instrument settings were used: ^{16}O primary beam, 10 nA beam current, 20 kV accelerating voltage, 20 μm beam diameter. Molecular interference (*e.g.*, $^{40}\text{Ca}^{16}\text{O}^+$ at $M/e = 56$) at masses 56(Fe), 85(Rb) and 88(Sr) require analysis at a mass resolution sufficient to separate the interference from the isotope of interest. These three isotopes were measured at a mass resolution of ~ 4100 . Careful high-resolution examination of various isotopes of the other elements showed them to be interference-free; thus ^7Li , ^{11}B , ^{19}F , ^{24}Mg , ^{31}P , ^{133}Cs , ^{138}Ba and ^{208}Pb were measured at low mass-resolution.

Standards were chosen for homogeneity and, where possible, high minor-element content (leading to favorable counting-statistics). Currently available calibrations indicate that yields of secondary ions for the elements studied are independent of major-element variations in alkali feldspars. Calibration of certain elements (*e.g.*, Rb) across the whole range of feldspar compositions is hampered by lack of suitable standards. The standards were checked periodically throughout a working day, and previous analyses discarded and repeated if the change in count rate for an element exceeded 5%. The analytical data are believed to be accurate to $\pm 25\%$ of the amount present. The precision is substantially better. At least some of the difference between ion- and electron-microprobe results for the same specimen come from variation from spot to spot, and from overlap with mechanical impurities.

The structural state of the feldspars was characterized mainly from X-ray powder diffractograms, using the procedure of Wright & Stewart (1968) and Bambauer *et al.* (1967). Single-crystal oscillation photographs were made for a few specimens of K-feldspar.

TEXTURAL AND STRUCTURAL CHARACTERISTICS OF THE FELDSPARS

Plagioclase

Polysynthetic albite-twinning is common in all plagioclase varieties. The lamellae are very narrow in cleavelandite (3) and (4) (Fig. 2b) and in saccharoidal albite (6); plagioclase (1), (1a) and (2) have broader lamellae, and the late varieties (5) and (7) in vugs and fissures consist of very few lamellae or a simple pair of individuals. Pericline twins are sparse and restricted to plagioclase (1), (1a) and (2). Compositional zoning seems to be absent in all plagioclase types, except for very thin and irregular rims of albite ($\sim \text{An}_3$) on the surface of plagioclase (1) and (2). Antiperthite is rare.

Although peristerite unmixing was not seen optically, Černý (1971) reported broadening of the 131 diffraction line. The powder patterns could be treated as representative of a single phase, and values of the 131 structural indicator (Fig. 3a) fall in the peristerite gap of ordered plagioclase (Bambauer *et al.* 1967). Because Or substitution displaces the 131 indicator to lower values, the near-contact plagioclase (1) and (1a) may be slightly disordered when corrected for the effect of $\sim 5\%$ Or.

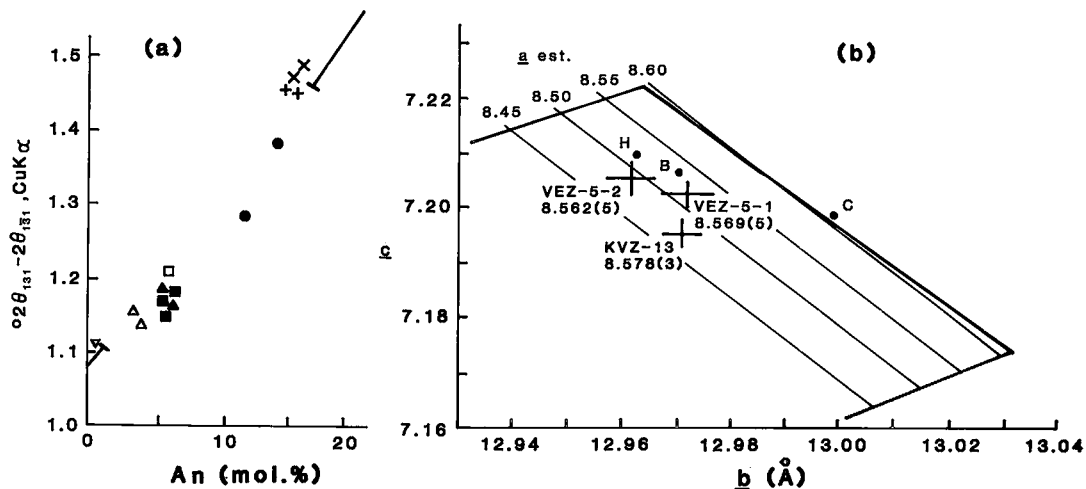


FIG. 3. Structural state of the feldspars. (a) $\Delta 131$ plot for plagioclases: line segments show the peristerite gap along the Bambauer *et al.* (1967) ordered low-temperature boundary. Plagioclase symbols as in Figure 1 and Table 2. (b) $a-b-c$ plot of the K-feldspar specimens from Table 2, with a (meas.) in Å; isopleths from Stewart & Wright (1974); reference samples H, B and C are ordered Himalaya orthoclase, Spencer's adularia B and orthoclase C, respectively.

K-feldspar

K-feldspar of all types is microperthitic, except adularia (7). The intergrowth varies from very fine string-perthite to a moderately coarse vein-perthite, commonly within the same crystal. The width of the albite veinlets ranges from 0.001 to 0.003 mm in string perthite and up to 0.1 mm in vein perthite (Fig. 4a,b). String albite is inclined at 104° and vein albite at 109° to (001) in sections parallel to (010) (Fig. 4d). Both types of perthitic plates of albite are within the $h0l$ zone, but the vein albite commonly deviates from this orientation (Fig. 4b). Extremely fine and homogeneous string perthite, which is slightly opalescent like moonstone in hand specimen, probably grades into cryptoperthite.

The potassic component of the perthite is mostly orthoclase, and exclusively so in string perthite. Incipient conversion to a triclinic K-feldspar is evident optically and by X-ray powder diffraction only in vein perthite (Fig. 4b). A single 131 peak of orthoclase in the string perthite becomes flanked by

variable but low-intensity shoulders of resolved 131 and $\bar{1}\bar{3}1$ reflections for vein perthite, indicating subordinate quantities of intermediate microcline with low triclinicity, generally less than 0.6 and only exceptionally reaching 0.8. Variable disorder prevents refinement of unit-cell dimensions from X-ray powder-diffraction data for most monoclinic and all triclinic phases.

Unit-cell dimensions of a moonstone-like microperthite KVZ-13 indicate an orthoclase structure considerably distorted by coherency strain (Table 1, Fig. 3b); $(a_{\text{obs}} - a_{\text{est}}) = 0.11 \text{ \AA}$ for this sample, using the method of Stewart & Wright (1974, Fig. 1). Orthoclase components of two samples of vein perthite have $(a_{\text{obs}} - a_{\text{est}})$ of 0.05 and 0.07 \AA , suggestive of coherency strain partly released by incipient conversion to microcline and twinning along the albite veinlets (Table 1, Fig. 4b). Unit-cell dimensions of these two orthoclase samples are close to those of the ordered Himalaya orthoclase (Prince *et al.* 1973) and the Spencer adularia B and orthoclase C (Colville & Ribbe 1968).

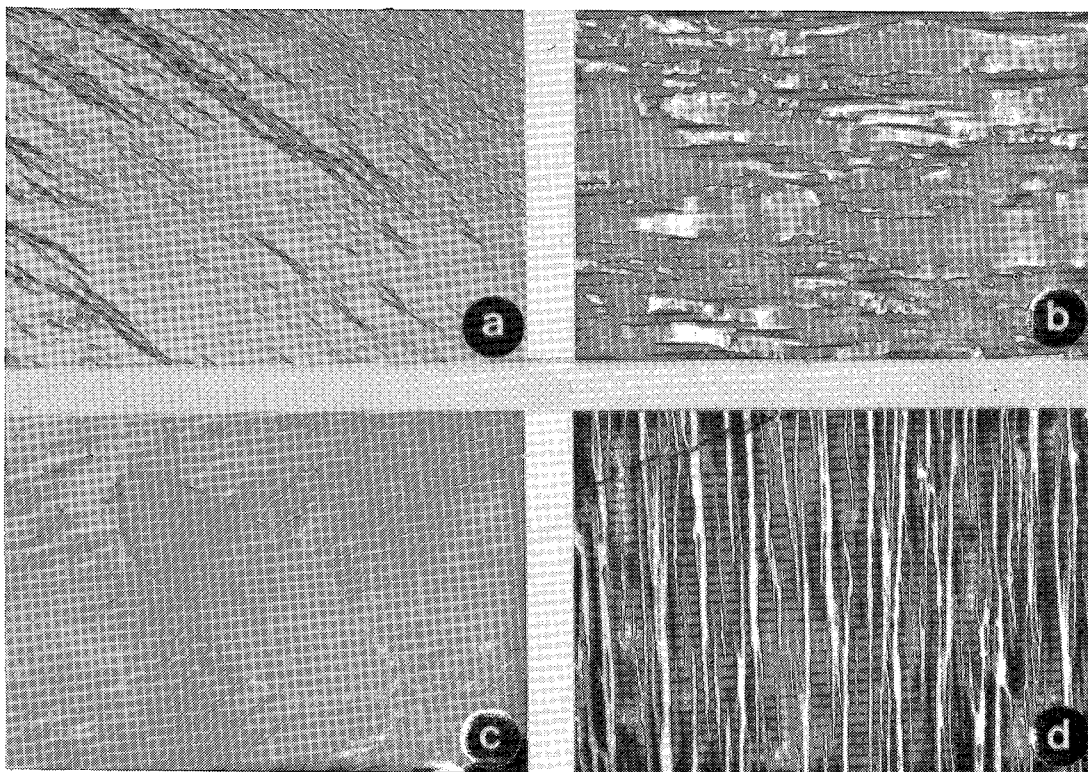


FIG. 4. Perthite textures. (a) String microperthite passing into vein perthite; section approximately // to (001), with the albite component at extinction. (b) Vein perthite with albite at extinction and the mottled birefringence typical of randomly disordered orthoclase to intermediate microcline; section // to (001). (c) Segregation of perthitic albite (white) along contacts with subgraphic quartz. (d) Variation in orientation of perthitic albite (white) relative to the (001) cleavage (upper left corner); section // to (010). The width of (a, b, d) is 2.5 mm; that of (c) is 5 mm.

TABLE 1. UNIT CELL DIMENSIONS OF K-FELDSPAR

Sample	KVZ-13*	V5-1**	V5-11**
a, Å	8.578(3)	8.569(5)	8.562(5)
b, Å	12.971(3)	12.972(5)	12.962(5)
c, Å	7.195(2)	7.202(3)	7.205(3)
β , °	116 ⁰ 2(1)'	116 ⁰ 1(2)'	116 ⁰ 1(2)'
V, Å ³	719.3(3)	719.4(5)	718.6(5)

*monoclinic micropertthitic K-feldspar.

**monoclinic component of a feldspar with variable order.

The distribution of the perthite types and of the concomitant variation in structural state of their potassic phase is rather variable but, in general, the vein perthite with incipient conversion to microcline tends to be more abundant in the central parts of the pegmatite, and at the rods of graphic quartz (Fig. 4c). Perthite segregation and formation of microcline are particularly evident close to fractures penetrated by saccharoidal albite (6) and associated rare-element mineralization. Late hydrothermal processes that gave rise to adularia (7) in open fissures did not have such an effect on the surrounding K-feldspar. The adularia is either monoclinic or a random mixture of monoclinic to intermediate triclinic (with a continuous range of triclinicity from 0 to 0.7).

Chips of perthitic K-feldspar separated from a single individual in the blocky intermediate zone, but displaying widely variable perthite texture and ordering, gave nearly identical bulk contents of Na and K (e.g., 10.45 wt. % K₂O in each of five fragments containing 4.25, 4.38, 4.38, 4.40 and 4.45 wt. % Na₂O). This homogeneity is consistent with formation of the perthites by exsolution in a chemical system closed on the scale of a centimetre, with the possible exception of regions containing late albite and cleavelandite. It will be assumed that the compositions derived by the partial atomic-absorption-spectrometry (AAS) analyses are representative of the original homogeneous crystals of K, Na-rich feldspar, and also of the plagioclase. The microprobe analyses of K-feldspar, however, pertain to regions free of vein albite and are necessarily biased toward the orthoclase component. For plagioclase, results of the electron-probe and AAS analyses are quite similar because of the rarity of antiperthitic K-feldspar.

CHEMICAL COMPOSITION OF THE FELDSPARS

The results of AAS (CaO, Na₂O, K₂O, Rb₂O) and electron-microprobe analyses (SiO₂, TiO₂, Al₂O₃, Fe₂O₃, CaO, Na₂O, K₂O, Rb₂O, BaO, SrO, P₂O₅) of the Věžná feldspars are presented in Tables 2 and 3. Ion-microprobe determinations of

some of the above elements and of additional ones present in low concentrations (Li, Mg, Cs, Pb, B, F) are given in Table 4. Concentrations of selected elements and ratios are illustrated in Figures 5 and 6.

Before discussing the details, it is desirable to cover general features in relation to the summaries in Smith (1974, Chapter 14) and Shmakin (1979). The extent of substitution of Mg, Ti and Fe is trivial in all the feldspars, especially for the former two elements; only Fe (presumably ferric) is consistently present at an average level of 0.01 wt. %. Phosphorus occurs in both feldspars (Fig. 6) at levels that have petrogenetic significance for the parent liquids. Most plagioclase contains about twice as much P as coexisting K-feldspar, and the late feldspars contain five times as much as the early ones. The former observation is indicative of a crystal-chemical control, and the latter is presumably the result of fractionation of P into a residual liquid. Even the highest value of 0.18 wt. % P₂O₅ in a saccharoidal albite is lower than the 0.33 wt. % for a late albite in the phosphate-bearing Dolní Bory pegmatite (Smith 1974, p. 63). The value of 0.25 wt. % P₂O₅ in a cavity K-feldspar is rather high for K-feldspar. The boron contents of 1–4 ppm are much lower than values collected in Smith (1974, p. 55), but are comparable with the range of 1–3 ppm in ion-probe analyses of anorthoclase (Mason *et al.* 1982).

Turning to the M sites, the extent of substitution of Rb, Sr, Ba (Fig. 6) and Cs is unremarkable in relation to the ranges for pegmatitic feldspars collected in Smith (1974). Furthermore, the data follow the general rule for pegmatites (e.g., Shmakin 1979) that Rb and Cs increase as Ba and Sr decrease from the earlier to the later generations of both K-feldspar and plagioclase. Barium, Rb and Cs are strongly fractionated into K-feldspar, whereas Sr is evenly partitioned between coexisting feldspars. The fractionation of Li is not understood. Lead is concentrated 4-fold into the early magmatic K-feldspar over the plagioclase, but may be erratically distributed in the later phases (*cf.* Smith 1974, p. 99).

A peak at mass 19 has been found in many silicates (I.M. Steele, pers. comm.); it seems necessary to ascribe it to fluorine. A calibration has not yet been obtained for the count rates reported in Table 4.

Plagioclase

Plagioclase compositions fall into several groups according to their paragenetic position: (i) primary plagioclase (1), (2) and (5), (ii) secondary cleavelandite (3) and (4), (iii) saccharoidal albite (6), (iv) fissure-grown hydrothermal albite (7), and (v) metasomatic contact plagioclase (1a).

Primary plagioclase (1) and (2) are relatively rich in Ca, Ba, Sr, K, Cs, Li and Fe but poor in Rb, P and B. Plagioclase (5) in the miarolitic cavities is

TABLE 2. ELECTRON MICROPROBE AND A.A.S. DATA FOR PLAGIOCLASE

SAMPLE	SiO ₂	TiO ₂	Al ₂ O ₃	Fe ₂ O ₃	CaO	Na ₂ O	K ₂ O	BaO	SrO	P ₂ O ₅	TOTAL
+ Wall zone granular plagioclase (1)											
PVZ-1	64.2	nd	22.6	0.009	3.01	9.08	0.91	0.034	0.051	0.023	99.917
					<i>3.09</i>	<i>8.87</i>	<i>1.13</i>				
PVZ-2	64.7	nd	22.1	0.010	2.87	9.03	0.96	0.038	0.048	0.026	99.782
					<i>3.03</i>	<i>8.50</i>	<i>1.05</i>				
PVZ-3	64.9	nd	22.7	0.018	2.79	9.20	0.75	0.030	0.045	0.024	100.457
					<i>2.83</i>	<i>8.47</i>	<i>1.23</i>				
PVZ-4	64.4	(0.002)	21.9	0.014	2.88	9.13	0.97	0.052	0.061	0.023	99.432
					<i>2.92</i>	<i>8.33</i>	<i>1.09</i>				
● Intermediate zone tabular plagioclase (2)											
PVZ-5	65.2	nd	22.2	0.018	2.77	9.35	0.86	0.033	0.049	0.024	100.504
					<i>2.84</i>	<i>9.48</i>	<i>1.07</i>				
PVZ-6	63.4	nd	21.6	0.012	2.40	9.55	0.99	0.042	0.054	0.029	98.119
					<i>2.81</i>	<i>8.13</i>	<i>1.21</i>				
▲ Graphic cleavelandite (3)											
C-1A	66.1	0.009	20.4	0.008	1.03	10.68	0.38	(0.001)	nd	0.102	98.710
					<i>1.15</i>	<i>10.52</i>	<i>0.89</i>				
C-101	67.1	nd	20.4	0.009	1.15	10.76	0.35	0.010	nd	0.118	99.897
					<i>1.36</i>	<i>10.16</i>	<i>1.13</i>				
C-102	67.0	(0.001)	20.6	(0.002)	1.17	10.69	0.32	0.009	nd	0.091	99.883
					<i>1.37</i>	<i>10.42</i>	<i>1.04</i>				
V-3	66.7	0.008	20.7	(0.008)	1.21	10.94	0.20	0.009	nd	0.099	99.874
					<i>1.53</i>	<i>9.86</i>	<i>1.56</i>				
V-4	66.4	nd	20.9	(0.002)	1.18	10.49	0.58	0.009	nd	0.076	99.637
					<i>1.34</i>	<i>9.75</i>	<i>1.88</i>				
NaGG-55					<i>1.29</i>	<i>9.89</i>	<i>1.77</i>				
NaGG-56					<i>1.03</i>	<i>10.43</i>	<i>1.23</i>				
NaGG-58					<i>1.04</i>	<i>10.25</i>	<i>1.33</i>				
NaGG-62					<i>0.99</i>	<i>10.15</i>	<i>1.46</i>				
■ Cleavelandite (4)											
PVZ-12	66.9	0.007	20.5	0.008	1.05	10.93	0.24	0.016	nd	0.103	99.754
					<i>1.08</i>	<i>10.00</i>	<i>1.27</i>				
PVZ-13	66.7	(0.003)	20.0	(0.003)	1.11	10.92	0.21	(0.003)	nd	0.146	99.095
					<i>1.17</i>	<i>10.33</i>	<i>1.42</i>				
PVZ-14	67.2	(0.005)	20.6	0.013	1.36	10.54	0.32	(0.006)	nd	0.087	100.131
					<i>1.22</i>	<i>10.13</i>	<i>1.49</i>				
V-1	67.3	(0.004)	19.5 ⁺	(0.007)	1.19	10.82	0.18	0.011	nd	0.093	99.105
					<i>1.24</i>	<i>10.21</i>	<i>1.38</i>				
V-2	66.4	nd	20.0	0.010	1.16	10.66	0.39	0.008	nd	0.089	98.717
					<i>1.13</i>	<i>10.51</i>	<i>1.08</i>				
□ Cavity plagioclase (5)											
PVZ-16A-2A	68.5 ⁺	(0.001)	19.6	(0.004)	0.06	11.5	0.18	0.015	nd	0.168	100.028
PVZ-17B	65.8	0.007	20.5	(0.002)	1.12	10.88	0.26	0.011	nd	0.146	98.726
					<i>1.02</i>	<i>10.62</i>	<i>0.59</i>				
PVZ-7					<i>0.84</i>	<i>10.95</i>	<i>0.37</i>				
△ Saccharoidal albite (6)											
PVZ-31	67.8	(0.001)	19.6	0.012	0.08	11.51	0.32	(0.003)	nd	0.093	99.419
					<i>0.12</i>	<i>11.50</i>	<i>0.53</i>				
PVZ-32	67.5 ⁺	nd	20.0 ⁺	0.012	0.80	10.78	0.15	(0.006)	nd	0.176	99.424
					<i>0.90</i>	<i>10.98</i>	<i>0.48</i>				
PVZ-33	65.4	nd	20.3	0.011	0.66	11.10	0.27	(0.006)	nd	0.134	97.881
					<i>0.72</i>	<i>11.00</i>	<i>0.40</i>				
PVZ-35					<i>0.32</i>	<i>11.33</i>	<i>0.22</i>				
PVZ-36					<i>0.21</i>	<i>11.28</i>	<i>0.26</i>				
▽ Late albite crystals (7)											
PVZ-37					<i>0.05</i>	<i>11.58</i>	<i>0.38</i>				
PVZ-38					<i>0.11</i>	<i>11.70</i>	<i>0.10</i>				
× Lower contact tabular plagioclase (1a)											
PVZ-8	63.7	nd	22.4	0.014	3.31	9.33	0.46	0.012	0.014	0.026	99.266
					<i>3.50</i>	<i>8.73</i>	<i>0.62</i>				
PVZ-9	64.1	nd	21.1	0.016	3.08	9.17	0.81	0.030	0.033	0.023	98.362
					<i>3.50</i>	<i>8.30</i>	<i>0.80</i>				
PVZ-10	64.2	nd	22.2	0.018	3.16	9.25	0.67	0.031	0.009	0.018	99.556
					<i>3.34</i>	<i>8.98</i>	<i>0.74</i>				
PVZ-11	64.1	nd	22.8	0.010	3.56	9.02	0.62	0.015	0.049	0.022	100.206
					<i>3.53</i>	<i>8.40</i>	<i>0.66</i>				

Electron-microprobe analyses by J. S. Delaney; A.A.S. analyses (*in italics*) by R. M. Hill and R. Chapman, University of Manitoba.

nd - not detected; quantities given in wt.%; + energy-dispersion data; () values within detection limits (2σ). MgO and Rb₂O not detected.

TABLE 3. ELECTRON MICROPROBE AND A.A.S. DATA FOR K-FELDSPAR

SAMPLE	SiO ₂	TiO ₂	Al ₂ O ₃	Fe ₂ O ₃	CaO	Na ₂ O	K ₂ O	Rb ₂ O	BaO	SrO	P ₂ O ₅	TOTAL
+ Wall zone granular K-feldspar (1)												
KVZ-1	63.6	nd	19.5	0.020	0.009	1.27	14.15	0.044	1.10	0.040	0.008	99.751
					<i>0.10</i>	<i>2.30</i>	<i>12.88</i>	<i>0.038</i>				
KVZ-2	64.3	nd	19.7	0.019	0.036	1.12	13.91	0.034	1.31	0.035	(0.006)	100.470
					<i>0.08</i>	<i>2.40</i>	<i>12.45</i>	<i>0.030</i>				
KVZ-3	64.8	nd	19.6	0.014	0.024	1.11	14.75	0.034	0.79	0.028	0.019	101.169
					<i>0.07</i>	<i>2.42</i>	<i>13.14</i>	<i>0.031</i>				
● Intermediate zone (graphic) K-feldspar (2)												
KVZ-4	64.5	nd	20.0	0.020	0.042	1.75	13.44	0.042	1.01	0.039	0.015	100.858
					<i>0.09</i>	<i>3.12</i>	<i>11.44</i>	<i>0.033</i>				
KVZ-5	64.6	nd	20.1	(0.001)	0.055	2.28	12.58	0.023	1.16	0.044	0.008	100.851
					<i>0.08</i>	<i>2.46</i>	<i>9.84</i>	<i>0.020</i>				
KVZ-6	63.6	nd	20.1	0.014	0.009	0.56	15.33	0.035	0.84	0.018	0.011	100.519
					<i>0.11</i>	<i>2.60</i>	<i>12.00</i>	<i>0.050</i>				
KVZ-7	64.1	nd	19.8	(0.004)	0.006	1.46	13.81	0.030	1.05	0.042	0.018	100.320
					<i>0.10</i>	<i>3.72</i>	<i>10.80</i>	<i>0.022</i>				
KVZ-13	65.9	nd	18.8 ⁺	0.012	0.083	2.16	13.34	0.34	1.14	0.046	0.007	101.522
					<i>0.13</i>	<i>3.54</i>	<i>12.00</i>	<i>0.031</i>				
KVZ-14					<i>0.06</i>	<i>2.92</i>	<i>12.20</i>	<i>0.043</i>				
▲ Graphic K-feldspar (3)												
KVZ-8	65.1	nd	19.4	0.011	0.014	1.21	15.22	0.086	0.060	nd	0.064	101.165
					<i>0.08</i>	<i>4.12</i>	<i>11.12</i>	<i>0.055</i>				
KVZ-9	64.7	nd	19.2	0.009	0.050	1.22	14.73	0.058	0.063	nd	0.041	100.071
					<i>0.09</i>	<i>3.88</i>	<i>11.35</i>	<i>0.051</i>				
KVZ-10	64.4	(0.002)	19.7	0.009	0.024	1.84	13.92	0.069	0.043	nd	0.034	100.041
					<i>0.08</i>	<i>4.46</i>	<i>10.80</i>	<i>0.059</i>				
KVZ-11	64.4	nd	19.7 ⁺	nd	0.098	3.60	10.95	0.013	1.14	0.039	0.008	99.948
					<i>0.13</i>	<i>4.09</i>	<i>11.25</i>	<i>0.040</i>				
KVZ-12					<i>0.14</i>	<i>3.88</i>	<i>11.40</i>	<i>0.041</i>				
KGG-18					<i>0.07</i>	<i>3.67</i>	<i>11.67</i>	<i>0.044</i>				
KGG-19					<i>0.06</i>	<i>4.07</i>	<i>11.26</i>	<i>0.053</i>				
KGG-21					<i>0.09</i>	<i>4.39</i>	<i>10.60</i>	<i>0.056</i>				
Kgg-22					<i>0.10</i>	<i>4.40</i>	<i>10.73</i>	<i>0.052</i>				
KGG-23					<i>0.07</i>	<i>3.99</i>	<i>11.42</i>	<i>0.049</i>				
KGG-24					<i>0.07</i>	<i>3.76</i>	<i>11.57</i>	<i>0.053</i>				
■ Blocky K-feldspar (4)												
KVZ-15	66.2	nd	18.9 ⁺	0.010	0.060	3.01	12.48	0.073	0.029	nd	0.066	100.828
					<i>0.10</i>	<i>4.28</i>	<i>11.04</i>	<i>0.080</i>				
KVZ-16	65.0 ⁺	nd	19.8	0.010	0.028	1.27	14.55	0.076	0.043	nd	0.054	100.831
					<i>0.09</i>	<i>4.15</i>	<i>10.88</i>	<i>0.056</i>				
KVZ-17	65.5 ⁺	0.008	19.0 ⁺	0.018	(0.004)	1.14	14.56	0.066	0.013	nd	0.071	100.384
					<i>0.08</i>	<i>4.58</i>	<i>10.80</i>	<i>0.047</i>				
KVZ-18	66.0 ⁺	0.011	19.0 ⁺	0.015	0.035	2.13	13.91	0.076	0.021	nd	0.101	101.309
					<i>0.10</i>	<i>4.36</i>	<i>10.80</i>	<i>0.058</i>				
KVZ-19	63.8	(0.004)	19.5	0.007	0.047	1.28	15.2 ⁺	0.069	0.027	nd	0.068	100.012
					<i>0.10</i>	<i>4.38</i>	<i>11.10</i>	<i>0.069</i>				
KVZ-20	63.8	nd	19.7	0.007	0.008	1.04	15.5 ⁺	0.076	0.038	nd	0.082	100.241
					<i>0.10</i>	<i>4.40</i>	<i>11.16</i>	<i>0.064</i>				
□ Cavity K-feldspar (5)												
KVZ-21	65.8	0.005	20.5	(0.004)	0.051	4.51	8.66	0.114	(0.005)	nd	0.251	99.900
					<i>0.07</i>	<i>3.80</i>	<i>11.48</i>	<i>0.095</i>				
KVZ-22	65.0 ⁺	0.019	19.7	0.025	0.053	2.19	15.0 ⁺	0.076	0.045	nd	0.092	102.200
					<i>0.08</i>	<i>4.26</i>	<i>10.61</i>	<i>0.078</i>				
KVZ-31					<i>0.03</i>	<i>4.60</i>	<i>10.22</i>	<i>0.097</i>				
▽ Adularia (7)												
KVZ-23					<i>0.02</i>	<i>0.78</i>	<i>15.40</i>	<i>0.059</i>				
KVZ-24					<i>0.06</i>	<i>0.52</i>	<i>15.70</i>	<i>0.098</i>				
KVZ-25	66.5	0.007	19.8	0.012	nd	0.062	14.02	0.061	0.020	nd	nd	100.482
					<i>0.01</i>	<i>0.40</i>	<i>16.26</i>	<i>0.054</i>				
KVZ-30	65.7	nd	20.2	0.027	0.008	1.31	12.17	0.084	0.029	nd	0.078	99.606
					<i>0.04</i>	<i>1.62</i>	<i>13.91</i>	<i>0.066</i>				

Electron-microprobe analyses by J. S. Delaney; A.A.S. analyses (*in italics*) by R. M. Hill and R. Chapman, University of Manitoba.
 nd - not detected; quantities given in wt.%; + energy-dispersion data; () values within detection limits (2 σ). MgO not detected.

TABLE 4. ION-MICROPROBE DATA FOR PLAGIOCLASE AND K-FELDSPAR

SAMPLE	Li	Rb	Cs	Mg	Sr	Ba	Pb	Fe	P	B	F*
Plagioclase											
+ PVZ-1	58	5	2.4	12	<i>400</i>	330	92	44	36	3.2	40
● PVZ-5	67	2	2.3	10	<i>400</i>	290	92	<i>100</i>	41	4.1	40
▲ C-101	19	2	0.08	9	21	9	108	26	500	7.6	50
■ V-1	19	1	0.06	25	21	7	77	9	550	12.7	40
□ PVZ-17	3.1	45	0.28	13	25	34	170	17	820	6.4	40
△ PVZ-32	1.2	1	0.18	113	17	26	115	<i>100</i>	730	7.6	40
× PVZ-10	23	2	0.74	17	340	105	15	<i>100</i>	27	3.5	40
K-feldspar											
+ KVZ-1	9	<i>400</i>	64	29	<i>300</i>	8600	550	<i>100</i>	68	12.7	10
● KVZ-5	53	200	62	18	<i>400</i>	8800	420	20	59	1.9	15
▲ KVZ-11	31	100	68	16	<i>300</i>	9900	440	40	64	1.9	15
■ KVZ-15	0.6	<i>700</i>	1.5	41	100	224	410	60	437	3.2	12
□ KVZ-22	0.4	<i>700</i>	2.8	74	60	380	61	<i>200</i>	127	3.2	0
▽ KVZ-25	0.05	<i>700</i>	1.0	34	60	158	0	75	14	1.9	0

Numbers *in italics*: electron-microprobe data by J. S. Delaney.
 Ion-microprobe analyses by R. A. Mason.
 Quantities given in ppm by weight except F*, for which counts/second are reported.

impoverished in the first group and relatively enriched in the second group of elements.

Cleavelandite (3) and (4) have overlapping compositional ranges except for singular extreme values of some elements (*cf.* K, Ba, P in Fig. 5). Compared to these feldspars, saccharoidal albite (6) is poorer in Ca, Ba and Li and enriched in P, but the differences in the other elements (higher Cs, Mg, (Fe?) and lower K) are only moderate. No significant difference is shown in the Rb, Sr, Pb, B and F contents.

The late hydrothermal albite (7), analyzed only by AAS, shows K contents similar to, but Ca lower than in the saccharoidal albite (6).

The metasomatic plagioclase (1a), located along the footwall contact with serpentinite, resembles somewhat the primary plagioclase (1) and (2). However, its K, Ba, Sr, Li, Cs and Pb contents are distinctly lower, and the Ca and P concentrations only slightly so.

K-feldspar

In bulk compositions of K-feldspar, the major alkalis change gradually throughout the primary zonal sequence; from (1) to (5), K and K/Na decrease, whereas Na increases. The considerable overlaps between the adjacent zones increase toward the centre of the pegmatite, but the overall trend is well defined (Fig. 5). K-feldspar crystals (5) from the miarolitic cavities coincide with the range of K-feldspar from both the graphic and blocky zones within which they occur. In contrast to the behavior of K and Na, a uniformly low level of Ca can be observed throughout the whole sequence from (1) to (5), oscillating within a narrow range of 0.08 wt. %.

Subordinate and trace elements show the following trends in the primary zonal sequence: Rb, Ti, P (and K/Ba) increase whereas Ba, Sr, Cs, Pb (and K/Rb and Ba/Rb) decrease. Two modes of behavior can be observed: Rb (and Pb?) contents and K/Rb ratios follow the relatively uniform and gradual change in Na and K/Na, whereas Ba, Sr, P concentrations and K/Ba, Ba/Rb (and probably Ba/Sr) ratios show a sharp break between types (2) and (3). [Sample KVZ-11 is the only one violating this generalization; this fine-grained K-feldspar + quartz graphic intergrowth is only 2-4 cm from the tabular subgraphic K-feldspar (2) sample KVZ-4]. The K-feldspar crystals (5) from miarolitic cavities have higher average contents of Rb and P, and lower K/Rb and Sr than do the neighboring feldspars (3) and (4).

Adularia (7) stands apart from most of the trends shown by K-feldspar, (1) to (5). Low Li, Rb, Cs, Na, Ca, Pb, P and B, and high K/Na and K/Rb are distinctive. Only the Ba, Sr and Fe contents and the K/Ba ratio seem to be comparable to the last generations of primary K-feldspar.

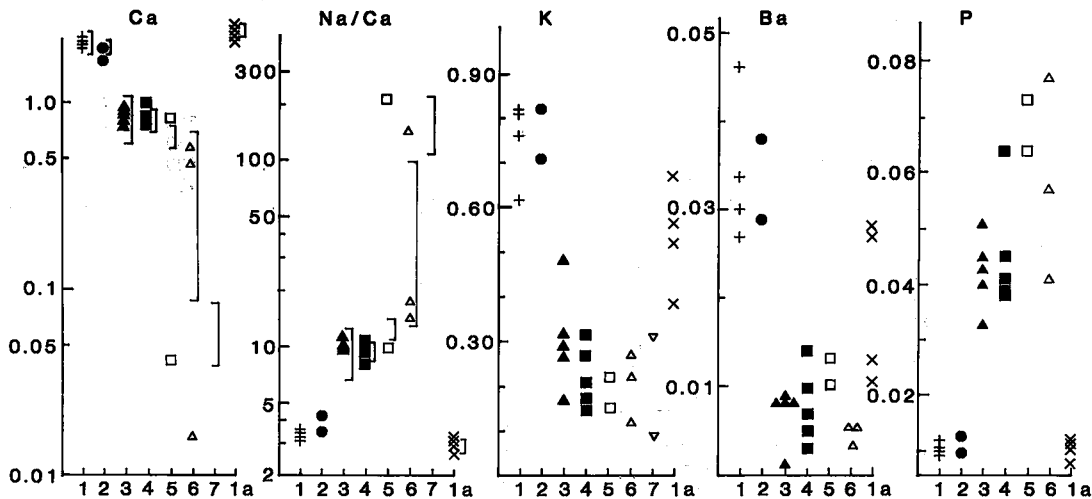
DISCUSSION

Paragenetic sequence of the feldspars

The generalized scheme of feldspar crystallization (Fig. 1b) is now discussed from the viewpoint of both textural and chemical data. Four features require comment:

(i) In the miarolitic cavities, plagioclase (5) is tentatively treated as contemporaneous with K-feldspar (5), although it may be later; its composition is close

PLAGIOCLASE



K-FELDSPAR

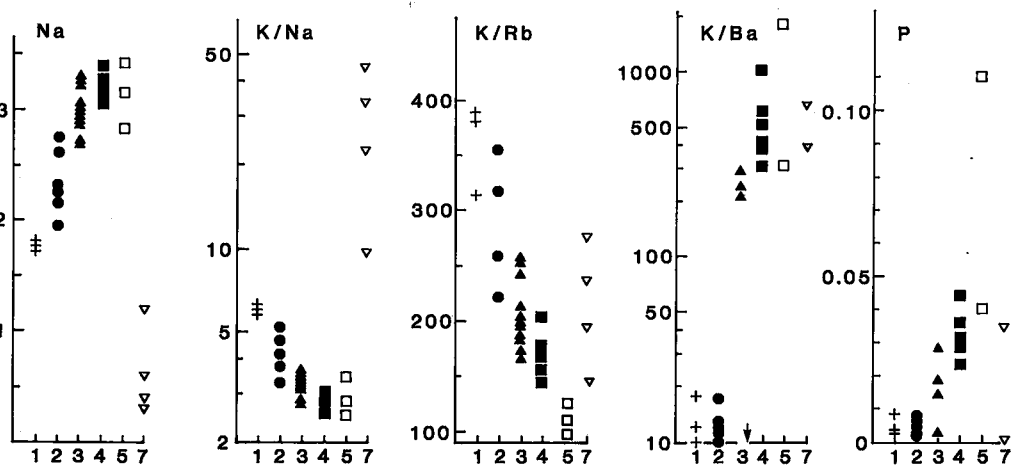


FIG. 5. Selected variations in chemical composition of the feldspars. The Ca, Na/Ca, K, Ba and P data points for plagioclase are from electron-microprobe results; the square brackets denote composition ranges shown by AAS analyses. The Na, K/Na and K/Rb diagrams for K-feldspar are from AAS bulk analyses, the K/Ba and P diagrams from electron-microprobe results. Feldspar symbols and assemblage numbers as in Figure 1 and Tables 2 and 3.

to that of cleavelandite (3) and (4), but identity with these types is not supported texturally.

(ii) In Figure 1(b), all the K-feldspar and plagioclase (5) from miarolitic cavities are marked as having crystallized after the precipitation of the blocky feldspar (4), although some of them probably crystallized somewhat earlier, in the vugs within the K-feldspar (3) of the inner graphic zone.

(iii) Cleavelandites (3) and (4) are virtually identical in texture and chemical composition, and differ only

in the presence of graphic quartz intergrown with cleavelandite (3). Since this cleavelandite + quartz intergrowth occurs only in the graphic K-feldspar + quartz zone, and since the quartz contents of both feldspars cover the same range (Fig. 7), all the quartz intergrown with cleavelandite (3) appears to be redeposited from quartz intergrown with the K-feldspar (3), as shown in Figure 2c. Thus the cleavelandites (3,4) are treated as a single generation.

(iv) The formation of a metasomatic assemblage of

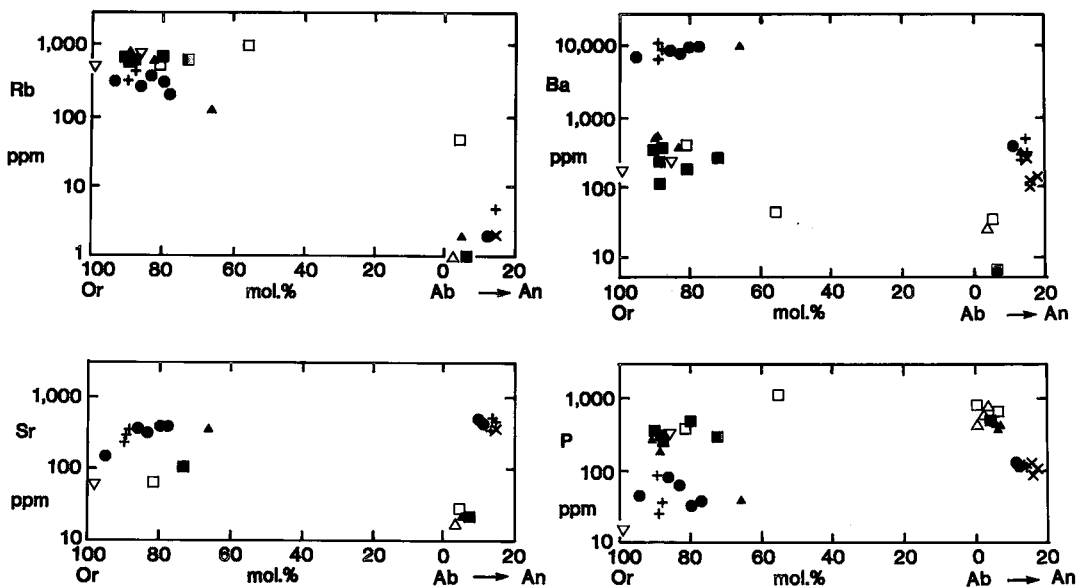


FIG. 6. Relations between minor and major elements in the feldspars. Minor elements Rb, Sr, Ba and P in ppm on log scale. Plagioclase is plotted in mol. % An and K-feldspar in mol. % Or. Symbols from Figure 1(a). Analytical data from Tables 2, 3 and 4. An arbitrary choice was made of some ion- and electron-microprobe analytical data.

plagioclase (1a) + phlogopite + apatite at the foot-wall contact of the pegmatite is tentatively correlated with the deposition of cleavelandite (3,4). The relative abundance of plagioclase (1a) matches that of the cleavelandite, and the absence of accessory mineralization separates it from the rare saccharoidal albite (6) associated with minerals of Be, B, Ti, Nb, Ta, Zr and REE.

The feldspar sequence illustrated in Figure 1(b) fits the generalized schemes of pegmatite crystallization derived by earlier authors. For the scheme of Ginzburg (1955, 1960), feldspars (1) and (2) correlate with the Na-Ca stage, and K-feldspars (3) and (4) with the K-stage of primary crystallization, whereas the metasomatic plagioclase (1a), (3), (4) and (6) belong to the metasomatic Na-stage and the fissure-hosted types (7) to the stage of late "alpine" crystallization.

Because several stages of albitization within a single pegmatite body were documented at many localities (e.g., Zalashkova 1957), the two generations of metasomatic albite at Věžná are not exceptional. The "alpine" origin of adularia (7) and albite (7) is not only indicated by their growth in open fissures and by their morphology, but it is also supported by their association with celadonite, secondary beryllium silicates and microlite that owe their origin to a hydrothermal decomposition of the earlier generations of feldspar and of beryl, beryllian cordierite and niobian rutile (Černý 1965, 1968a). Hydrothermal leaching of wallrock (represented in this case by

the pegmatite) and precipitation of mobilized components in open fractures are the principal mechanisms involved in the formation of alpine-type mineral veins.

Geochemical evolution of the feldspars

In terms of the ternary system Or-Ab-An, successive generations of plagioclase show a progressive decrease in both An and Or (except 1a, Fig. 8). A conspicuous difference in An separates the primary plagioclase (1), (2) and secondary plagioclase (1a) at the pegmatite margins from the internally located albite. Near-contact contamination by the reaction with the serpentinite host (1.4–2.2 wt.% CaO) is probably responsible. Despite the lack of mass-balance estimates, only a small fraction of the Ca mobilized during the contact reaction seems to be bound in the accessory tremolite and apatite. Such an explanation of the Ca-enriched plagioclase is in agreement with Ginzburg (1955, 1960), who ascribed the extent of the initial (Na,Ca)-stage in complex pegmatites mainly to the degree of Ca assimilation from the wallrocks. It also agrees with the observation that pegmatites geochemically similar to the Věžná body and intruded into granitic and trondhjemitic gneisses lack plagioclase with An > 10, even along contacts (Černý, unpubl. data).

The primary K-feldspar displays a steadily declining Or/Ab ratio, whereas the negligible An content,

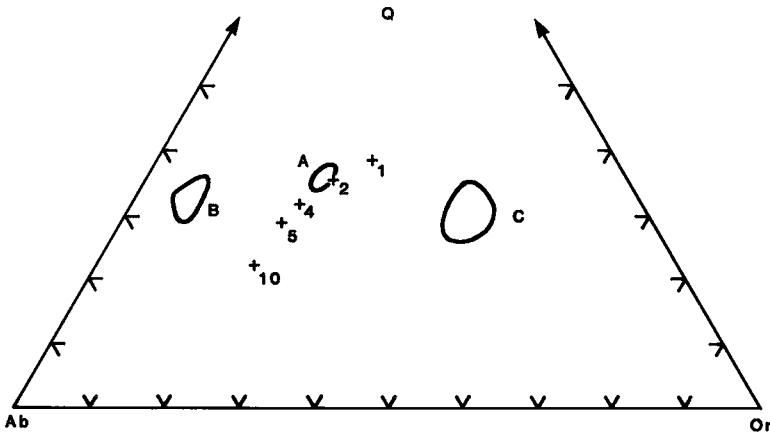


FIG. 7. Composition of the two-feldspar + quartz wall zone (A; 3 samples), cleavelandite + quartz graphic intergrowth (B; 10 samples) and K-feldspar + quartz graphic intergrowth (C; 9 samples) in the Ab-Or-Q diagram. Pseudoternary minima and eutectics at 1 to 10 kbar after Tuttle & Bowen (1958) and Luth *et al.* (1964).

averaging 0.4 wt.%, remains virtually constant. High Or/Ab and very low An are typical of the late adularia (7).

Most of the trace elements follow fractionation trends expected from the rules of Goldschmidt (1937) and Ringwood (1955). Barium and Sr decrease in the plagioclase, whereas Rb, K/Ba increase and Ba, Sr, K/Rb, Ba/Rb (and Ba/Sr?) decrease in the K-feldspar. Lead is notorious for its mobility in solutions and occasionally erratic distribution in feldspars (Smith 1974, p. 99-105), partly influenced by the activity of S^{2-} . Thus it is not surprising that the data in Table 4 do not define any obvious pattern.

The apparent decrease in Cs with progressing crystallization (Table 4) is puzzling in view of abundant evidence from pegmatites that Cs is even more strongly fractionated into a residual melt than Rb (*e.g.*, Goad & Černý 1981), and of confirmatory evidence from laboratory experiments (*e.g.*, Carron & Lagache 1980). Such a depletion in Cs might possibly be expected in late generations of K-feldspar equilibrated with muscovite. Cesium would partition strongly into the mica structure. However, muscovite is extremely rare in the Věžná pegmatite, and its small flakes are associated with saccharoidal albite and rare-element minerals. Moreover, increase in Cs is commonly observed throughout the interval of K-feldspar crystallization, even in pegmatites that carry apparently coexisting K-feldspar and Cs-enriched mica in their inner zones (Černý *et al.* 1981, Černý 1982b).

Because the Věžná pegmatite has a very low content of phosphate minerals (apatite and rare monazite, mostly in late-stage metasomatic assemblages), it is possible that the P content of the

primary feldspars is lower than in feldspars from phosphate-rich pegmatites (*cf.* Dolní Bory pegmatite listed earlier). Detailed microprobe analyses are needed for a range of feldspars from different paragenetic and geochemical types of pegmatite, particularly from the phosphate-rich types that were shown to contain as much as 1.1 wt.% P_2O_5 in wet-chemical analyses of optically homogeneous feldspars (Strunz *et al.* 1975).

Special microprobe analyses are needed of fresh areas of feldspars to determine whether they are peraluminous and cation-deficient. Such compositions are to be expected in view of the generally peraluminous bulk compositions of pegmatite (*e.g.*, Černý 1982a). Particular emphasis should be placed on ion-probe and infrared-absorption (Solomon & Rossman 1979) determinations of H that might be charge-balanced with some Al. The proposed $P + Al = 2Si$ substitution (Simpson 1977) could account for only 1% at most of the Al in the Věžná feldspars.

P, T estimates

A water pressure of 2.5 ± 0.5 kbar might be inferred from the mean An-free composition of $Ab_{41}Or_{23}Q_{36}$ for wall-zone samples of coexisting K-feldspar + plagioclase + quartz (area A, Fig. 7; *cf.* Anderson & Cullers 1978, Fig. 7). The occurrence of cordierite in the Věžná pegmatite and apparently primary andalusite in nearby pegmatites is consistent with a pressure lower than that for the peak of regional metamorphism of amphibolite grade. Tectonic emplacement of harzburgite followed by *in situ* serpentinization during unloading and cooling

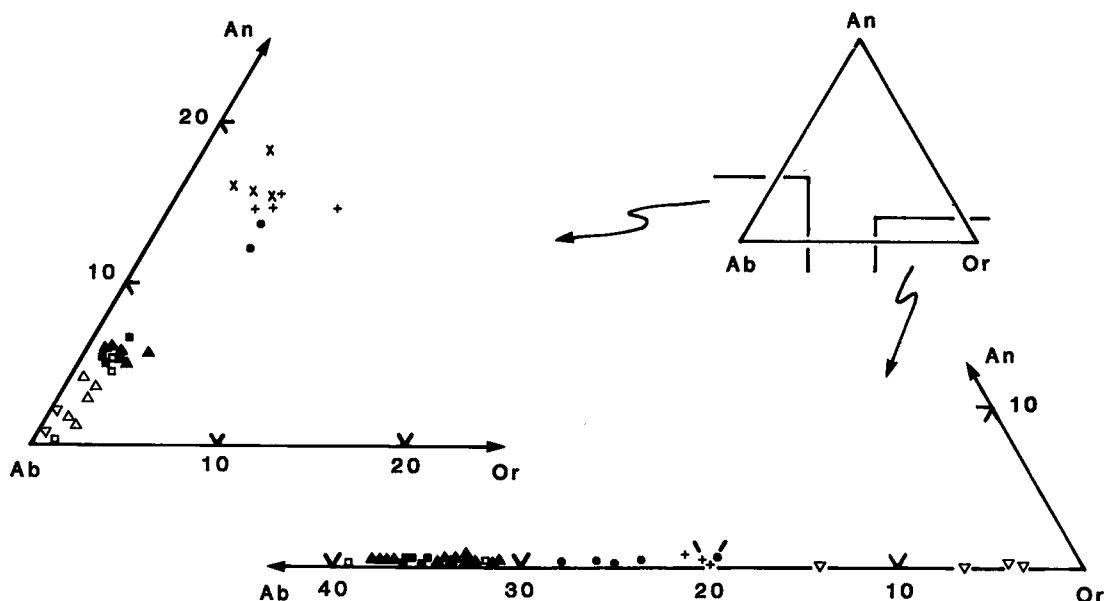


FIG. 8. Feldspar compositions in the Ab-An-Or diagram. Plagioclase plots from the electron-microprobe data are complemented by a few samples for which only the AAS results are available; bulk compositions of K-feldspar were determined by AAS. Feldspar symbols correspond to those of Figure 1 and Tables 1 and 2.

to $\sim 350^{\circ}\text{C}$ (Černý 1965) apparently preceded emplacement of pegmatite into a low-pressure fracture.

Two-feldspar thermometry is qualitatively useful, but quantification is difficult because of problems of metastable crystallization and complex thermodynamic formulation (Brown & Parsons 1981); furthermore, the extent of subsolidus interchange and of metasomatism is difficult to determine. It will suffice to say that the compositions of the primary-textured feldspars are not inconsistent with primary crystallization in a narrow range of temperature between those for "wet" haplogranite ($730\text{--}660^{\circ}\text{C}$) and Harding Li-pegmatite ($670\text{--}560^{\circ}\text{C}$) at 2.5 kbar water pressure (cf. Vaughan 1963, Luth *et al.* 1964, Jahns 1982), as would be expected for the relative amounts of components that depress the solidus. A range between 700 and 600°C appears to be a realistic estimate. The rather pure varieties of adularia and albite in the fissures indicate rather low temperatures in the order of 350 to 250°C , as for adularia in Alpine veins (*e.g.*, Nissen 1967).

Another estimate of temperature may be derived from the 1.77 wt.% BeO content of cordierite, crystallized in a Na- and Be-saturated environment (Černý & Povondra 1966). Interpolated from experimental data obtained by Povondra & Langer (1971) at 1 and 3 kbar $\text{P}(\text{H}_2\text{O})$, the minimum temperature at 2.5 kbar $\text{P}(\text{H}_2\text{O})$ would be about 590°C , based on the stability of pure Mg-cordierite. This

estimate may be shifted to lower temperatures by the presence of Fe, and probably also (Na, Be). Precipitation of the beryllian cordierite at less than about 590°C would be compatible with the temperature range of crystallization of the primary feldspars in general, and with the crystallization of blocky and vug feldspars in particular.

Petrogenesis of the feldspars

As evident from Martin's (1982) review and from the introduction to the present paper, there are virtually no studies available in the literature that deal with the compositional evolution of feldspar sequences throughout the complete crystallization of a pegmatite. Difficulties in acquisition of representative data, and the deterrent effect of disequilibria, replacements and low-temperature re-equilibrations demonstrated in studies of restricted feldspar assemblages probably are responsible for this lack of research.

The Věžná pegmatite was selected to open the present series of feldspar studies mainly because of its relatively simple zoning and feldspar assemblages, and because the textural and phase constitution of the feldspars suggest close correspondence between their composition at the time of crystallization and their present bulk-chemistry. Nevertheless, petrological interpretation of the feldspar compositions shown in Figure 8 is far from simple, and even a cur-

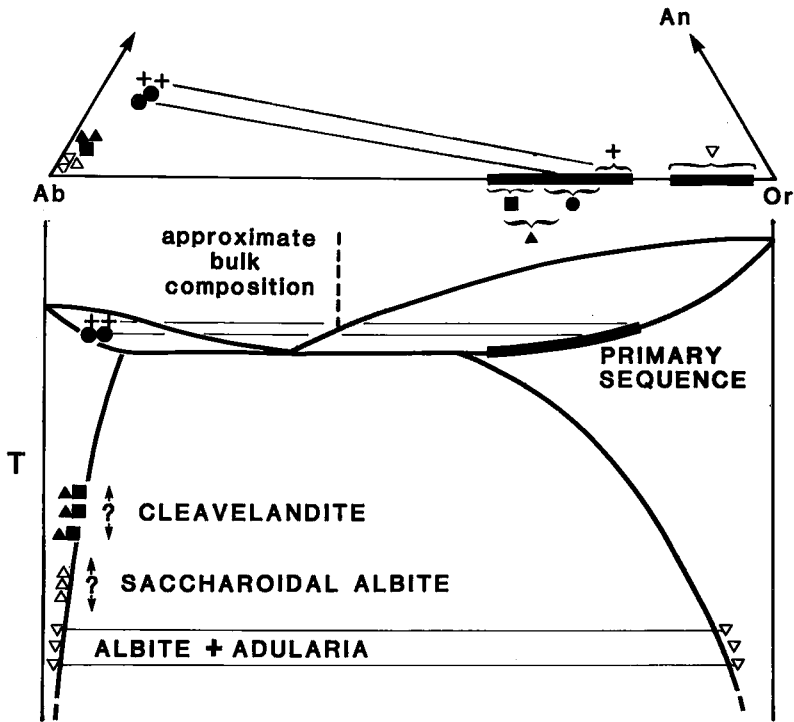


FIG. 9. Model of feldspar crystallization based on the sequence of feldspar assemblages, bulk compositions (schematized at the top from Fig. 8), and limited intersection of the binary solidus and solvus. In the T-X diagram, plagioclase compositions and a pseudobinary section are projected onto the Ab-Or-T plane. The position of the solvus in the pseudobinary section is arbitrary; this is particularly the case for the sodic boundary, which may be affected strongly by the structural state of the albite solid-solution and by the An content. See text for detailed discussion.

sory inspection reveals significant deviations from simple paths of crystallization in terms of the ternary system Ab-Or-An as well as the alkali feldspar system. Contact reaction with the serpentinite wall-rock undoubtedly affects some of the feldspar compositions, but cannot be responsible for the proportion of K, Na and Ca in the feldspars within the pegmatite, away from its margins.

The model proposed here is based on the principle of crystallization from an alkali feldspar system in the presence of quartz and H₂O, locally disturbed by introduction of Ca from the wallrock, and on the identity between the present bulk-chemistry of the feldspars and their composition at the time of crystallization. The key element is the almost An-free sequence of the primary K-feldspar, constituting the bulk of the pegmatite, which ranges from Or₈₀Ab₂₀ at the margins to Or₆₂Ab₃₈ at the core (Fig. 8). This sequence can be interpreted in terms of fractional crystallization in the system Ab + Or + Q + H₂O,

from a bulk composition within the span of the K-feldspar liquidus - solidus loop (Fig. 9).

The solidus part of the loop is quite extensive, since the estimated pressure of 2.5 kbar is considered the lowest one at which the alkali-feldspar solidus and solvus in the haplogranite + H₂O system may intersect (Stewart & Roseboom 1962, Morse 1970, Martin & Bonin 1976). The intersection should be, however, somewhat extended by the presence of components other than H₂O that depress the solidus, such as F and P₂O₅. The liquidus part of the loop overlaps the bulk feldspar compositions typical for granitic pegmatites, Ab₆₅Or₃₅ to Ab₅₅Or₄₅ [Černý (1971), based on data by Orville (1960) and Luth *et al.* (1964)]. The pressure of the haplogranite solidus - alkali feldspar critical curve intersection may be even higher for peraluminous feldspars (Seck 1972, Luth *et al.* 1974). Thus the primary K-feldspar sequence studied here has a hypersolvus character; the shallow thermal gradient of the K-feldspar soli-

dus and probable temperature variations along the pegmatite vein may explain the compositional overlaps of the K-feldspar from different pegmatite zones.

Coprecipitation of plagioclase (1) and (2) in the early stages of the K-feldspar crystallization may be explained as a restricted, marginal contamination effect, not influencing the bulk of the pegmatite melt. The very limited extent of plagioclase crystallization and the fact that the coexisting K-feldspar is not Ca-enriched relative to the later generations suggest that equilibrium was not achieved within the local Or–Ab–An–Q–H₂O system generated by assimilation of Ca along contacts.

The above interpretation appears to fit the observed data better than other possible modes of origin. Martin & Bonin (1976, p. 233) theorized that "hypersolvus mineralogy can form at total pressures well above 2.5 kbar if P(H₂O) is maintained at low value," because of a considerable increase in solidus temperature, which expands the temperature gap between the solidus trough and solvus crest. This condition, however, is difficult to expect in volatile-rich pegmatite melts. Tuttle & Bowen (1958, p. 134) showed that early coprecipitation of two feldspars from a relatively Ca-rich melt may be followed by crystallization of K-feldspar only (*cf.* also Stewart & Roseboom 1962, Abbott 1978). In our case, however, the pairs of early feldspar do not appear to have crystallized from a melt representative of the whole pegmatite, and the blocky crystals of K-feldspar (4) appear to be not sufficiently sodic for the cases illustrated by the above authors.

Compositions of the feldspars (5) from the miarolitic cavities, Or₂Ab_{92-97.8}An_{0.2-6} and Or_{64.5}Ab₃₅An_{0.5}, suggest that they either are unequilibrated coprecipitates terminating the primary crystallization at the solidus–solvus intersection or they belong to different feldspar generations, as considered earlier.

The An-, Or-poor metasomatic albite (3, 4) and (6) could form in the subsolidus region outside the binary and ternary solvi, since they are not associated with a coexisting K-feldspar (Fig. 9). This is a general characteristic of albitization in granitic pegmatites, a process generated by supercritical to hydrothermal, Na-enriched and relatively low-pH fluids, separated during the crystallization of volatile-oversaturated melts. Re-equilibration of these fluids at subsolidus temperatures with the solid phases (in conjunction with the breakdown of rare-element-bearing complexes and coprecipitation of Be-, Nb-, Ta-, Ti-, Zr-bearing minerals: Beus 1961, Beus *et al.* 1963) leads to replacement of K-feldspar by albite and formation of hydrolytic muscovite, or complete flushing out and dispersion of K. Local enrichment of the metasomatic albite in An, such as in type (1a), is understandable because of the mobility of the albitizing fluids within the small pegmatite body, which

brings them into an occasional contact with the Ca-bearing wallrock.

The "alpine" feldspars (7) in the open fissures are typical hydrothermal phases in the Or–Ab–Q–H₂O system, concluding the feldspar crystallization at low subsolidus temperatures (Fig. 9). The predominance and the commonly exclusive presence of adularia in this assemblage may be explained by significant reduction of P_{fluid} upon the opening of fissures, with consequent unmixing of the hydrothermal fluid into liquid + gas, and a shift to lower K/(K + Na) in its bulk composition, which forces precipitation of K-feldspar (Lagache & Weisbrod 1977).

CONCLUDING REMARKS

It would be premature to extrapolate the results of the present investigation, which is in many respects a pioneering one, to other pegmatites. Generalizations will be possible only after additional studies of similar pegmatites as well as other paragenetic and geochemical types of pegmatite. Nevertheless, some aspects of the foregoing results deserve more general comment.

The model presented above for the primary igneous crystallization of the feldspars, producing predominantly (to exclusively) potassic zones and consequently drastically reducing the K/(K + Na) ratio in residual subsolidus fluids, may be applicable to a variety of other pegmatite types. Many Ca-poor granitic pegmatites with relatively simple zoning and geochemistry display a sequence of primary K-feldspar, which becomes penetrated by albite only in later metasomatic events.

In the generations of primary K-feldspar in the Věžná pegmatite, the gradual change in K/Na and K/Rb is in conspicuous contrast with the break in the K/Ba, P (Fig. 5) (and, probably, Sr) trends. The discontinuity occurs at the boundary of the wall and intermediate graphic zones. Future examination of similar pegmatites located in host rocks of granitoid composition should show whether this break is a persistent feature reflecting internal changes in physicochemical conditions (onset of separation of a supercritical fluid?) or an effect of contact reaction and chilling.

Another problem of general significance is the nature of cleavelandite in general, and of the graphic cleavelandite + quartz intergrowths in particular. In an earlier study of graphic feldspar + quartz intergrowths from a multitude of localities, cleavelandite + quartz was treated as contemporaneous with K-feldspar + quartz, both intergrowths appearing as compositional complements during simultaneous crystallization along ternary feldspar solidus–solvus intersection in the quinary system Ab–An–Or–Q–H₂O (Černý 1971). This interpretation, prompted by a relatively high K-content of cleavelandite and Ca-

content of K-feldspar, proved erroneous in the course of subsequent studies reported in the present paper. For the Věžná pegmatite, the compositional identity of cleavelandite with and without graphic quartz is established here beyond reasonable doubt. The cross-cutting and metasomatic relationships observed in the field and microscopically for both of these varieties of cleavelandite support their late origin with respect to the graphic and blocky K-feldspar. Nevertheless, many thin sections from Věžná and other pegmatites reveal simple contacts between K-feldspar- and cleavelandite-based graphic intergrowths, with no indication of replacement and with quartz rods differently shaped, but optically oriented uniformly in both feldspar hosts. Also, cleavelandite is well known to form rims surrounding crystals of K-feldspar, spodumene, petalite and amblygonite, slightly corroding but mainly overgrowing them. A "neocrystallization" is evidently involved here, with negligible, if any, alkali metasomatism within an "immobile" Si, Al matrix. A need for a thorough study of different varieties of cleavelandite from different pegmatite types and mineral assemblages is clearly indicated.

Finally, the question of the nonequilibrium composition of feldspars documented here for coexisting pairs from the wall and inner graphic zones should be addressed. In the case described, disequilibrium appears to be the result of chilling and spatially limited enrichment of Ca in plagioclase adjacent to the pegmatite contact. Rapid crystallization from an undercooled medium may be typical of the graphic zones in general (Fenn 1979), and should promote compositional disequilibrium in the precipitating feldspars. Contrary to the earlier views of giant crystals of pegmatite minerals as products of slow crystallization, the ubiquitous presence of graphic intergrowths of rock-forming and accessory silicates with quartz is more recently interpreted as products of high crystallization rates in a relatively viscous medium (Martin 1982). Under these conditions, attainment of equilibrium in feldspar assemblages is not likely, and metastable compositions of feldspars may be the rule rather than the exception.

ACKNOWLEDGEMENTS

This study was supported by the NSERC of Canada operating grant A-7948, the NSF grants EAR 77-08100 and 80-23444 in support of R.A.M. and J.D.S., and the NASA 14-001-171 and NSF DMR grants supporting the electron- and ion-microprobe laboratories at the University of Chicago. The AAS analyses were performed by R.M. Hill and R. Chapman at the Department of Earth Sciences, University of Manitoba. Technical assistance from I.M. Steele, I.D. Hutcheon, O. Draughn, R. Draus and N. Weber at the University of Chicago is also acknowledged. Comments by two

anonymous referees and careful editing of the manuscript by R.F. Martin and E.E. Foord are greatly appreciated.

REFERENCES

- ABBOTT, R.N., JR. (1978): Peritectic reactions in the system An-Ab-Or-Qz-H₂O. *Can. Mineral.* **16**, 245-256.
- ANDERSON, J.L. & CULLERS, R.L. (1978): Geochemistry and evolution of the Wolf River batholith, a late Precambrian rapakivi massif in north Wisconsin, U.S.A. *Precamb. Res.* **7**, 287-324.
- BACHINSKI, S.W. & ORVILLE, P.M. (1969): Experimental determination of the microcline - low albite solvus and interpretation of the crystallization history of perthites. *Geol. Soc. Amer. Spec. Pap.* **121**, 15.
- BAMBAUER, H.U., CORLETT, M., EBERHARD, E. & VISWANATHAN, K. (1967): Diagrams for the determination of plagioclases using X-ray powder methods. *Schweiz. Mineral. Petrog. Mitt.* **47**, 333-349.
- BEUS, A.A. (1961): Acidity-alkalinity relationships in metasomatism as a factor of migration and concentration of rare elements. *D. S. Korzhinsky Anniv. Vol., Acad. Sci. U.S.S.R.*, 149-160 (in Russ.).
- _____, SOBOLEV, B.P. & DIKOV, YU. P. (1963): Geochemistry of beryllium in high temperature post-magmatic mineralization. *Geochem.*, 316-323.
- BROWN, W.L. & PARSONS, I. (1981): Towards a more practical two-feldspar geothermometer. *Contr. Mineral. Petrology* **76**, 369-377.
- CARL, J.D. (1962): An investigation of minor element content of potash feldspar from pegmatites, Haystack Range, Wyoming. *Econ. Geol.* **57**, 1095-1115.
- CARRON, J.-P. & LAGACHE, M. (1980): Étude expérimentale du fractionnement des éléments Rb, Cs, Sr et Ba entre feldspaths alcalins, solutions hydrothermales et liquides silicatés dans le système Q•Ab•Or•H₂O à 2 kbar entre 700 et 800°C. *Bull. Minéral.* **103**, 571-578.
- ČERNÝ, P. (1965): *Mineralogy of Two Pegmatites from Věžná*. Ph.D. thesis, Geol. Inst., Czech. Acad. Sci., Prague (in Czech).
- _____, (1968a): Berylliumminerale in Pegmatiten von Věžná und ihre Umwandlungen. *Ber. Dtsch. Ges. Geol. Wiss. B* **13**, 565-578.
- _____, (1968b): Comments on serpentinization and related metasomatism. *Amer. Mineral.* **53**, 1377-1385.

- ____ (1971): Graphic intergrowths of feldspars and quartz in some Czechoslovak pegmatites. *Contr. Mineral. Petrology* **30**, 343-355.
- ____ (1982a): Anatomy and classification of granitic pegmatites. In *Granitic Pegmatites in Science and Industry* (P. Černý, ed.). *Mineral. Assoc. Can., Short Course Handbook* **8**, 1-39.
- ____ (1982b): The Tanco pegmatite at Bernic Lake, southeastern Manitoba. In *Granitic Pegmatites in Science and Industry* (P. Černý, ed.). *Mineral. Assoc. Can., Short Course Handbook* **8**, 527-543.
- ____, ČECH, F. & POVONDRA, P. (1964): Review of ilmenorutile-strüverite minerals. *Neues Jahrb. Mineral. Abh.* **101**, 142-172.
- ____ & MACEK, J. (1972): The Tanco pegmatite at Bernic Lake, Manitoba. V. Coloured potassium feldspars. *Can. Mineral.* **11**, 679-689.
- ____ & ____ (1974): Petrology of potassium feldspars in two lithium-bearing pegmatites. In *The Feldspars* (W.S. MacKenzie & J. Zussman, eds.). Proc. NATO Adv. Study Inst. (Manchester 1972). Manchester Univ. Press, England.
- ____ & MIŠKOVSKÝ, J. (1966): Ferroan phlogopite and magnesium vermiculite from Věžná, western Moravia. *Acta Univ. Carolinae - Geol.*, **1**, 17-32.
- ____ & POVONDRA, P. (1966): Beryllian cordierite from Věžná: (Na,K) + Be → Al. *Neues Jahrb. Mineral. Monatsh.*, 36-44.
- ____, TRUEMAN, D.L., ZIEHLKE, D.V., GOAD, B.E. & PAUL, B.J. (1981): The Cat Lake - Winnipeg River and the Wekusko Lake pegmatite fields, Manitoba. *Man. Mineral Res. Div., Econ. Geol. Rep.* **ER80-1**.
- COLVILLE, A.A. & RIBBE P.H. (1968): The crystal structure of an adularia and a refinement of the structure of orthoclase. *Amer. Mineral.* **53**, 25-37.
- CORREIA NEVES, J.M. (1964): Genese des zonar gebauten Beryllpegmatits von Venturinha (Viseu, Portugal) in geochemischer Sicht. *Beitr. Mineral. Petrology* **10**, 357-373.
- FENN, P.M. (1979): On the origin of graphic intergrowths. *Geol. Soc. Amer. Abstr. Programs* **11**, 424.
- FISHER, D.J. (1971): Poikilitic albite in the microcline of granitic pegmatites. *Amer. Mineral.* **56**, 1769-1787.
- FOORD, E.E. (1976): *Mineralogy and Petrogenesis of Layered Pegmatite-Aplite Dikes in the Mesa Grande District, San Diego County, California*. Ph.D. thesis, Stanford Univ., Stanford, California.
- ____ & MARTIN, R.F. (1979): Amazonite from the Pikes Peak batholith. *Mineral. Record* **10**, 373-384.
- GINZBURG, A.I. (1955): Mineralogical and geochemical characteristics of lithium pegmatites. *Mineral. Museum Acad. Sci. U.S.S.R. Trans.* **7**, 12-55 (in Russ.).
- ____ (1960): Specific geochemical features of the pegmatitic process. *Int. Geol. Congress 21st (Norden)* **17**, 111-121.
- GOAD, B.E. & ČERNÝ, P. (1981): Peraluminous pegmatitic granites and their pegmatite aureoles in the Winnipeg River district, southeastern Manitoba. *Can. Mineral.* **19**, 177-194.
- GOLDSCHMIDT, V.M. (1937): The principles of distribution of chemical elements in minerals and rocks. *J. Chem. Soc.*, 655-672.
- GORDIYENKO, V.V. (1964): On rubidium microcline from pegmatite veins of the sodium-lithium type. *Zap. Vses. Mineral. Obshchest.* **93**, 281-288 (in Russ.).
- ____ (1971): Concentrations of Li, Rb, and Cs in potash feldspar and muscovite as criteria for assessing the rare-metal mineralization in granite pegmatites. *Int. Geol. Rev.* **13**, 134-142.
- ____ (1976): Diagrams for predictions and evaluation of rare-metal mineralization in granitic pegmatite from variations in composition of potassium feldspars. *Dokl. Acad. Sci. U.S.S.R., Earth Sci. Sect.* **228**, 149-151.
- HEIER, K.S. & TAYLOR, S.R. (1959): Distribution of Li, Na, K, Rb, Cs, Pb and Tl in southern Norwegian pre-Cambrian alkali feldspars. *Geochim. Cosmochim. Acta* **15**, 284-304.
- JAHNS, R.H. (1982): Internal evolution of granitic pegmatites. In *Granitic Pegmatites in Science and Industry*, (P. Černý, ed.). *Mineral. Assoc. Can., Short Course Handbook* **8**, 293-346.
- KRETZ, R. (1970): Variation in the composition of muscovite and albite in a pegmatite dike near Yellowknife, N.W.T. *Can. J. Earth Sci.* **7**, 1219-1235.
- LAGACHE, M. & WEISBROD, A. (1977): The system: two alkali feldspars - KCl - NaCl - H₂O at moderate to high temperatures and low pressures. *Contr. Mineral. Petrology* **62**, 77-101.
- LAPPALAINEN, R. & NEUVONEN, K.J. (1968): Trace elements in some Finnish pegmatitic potassium feldspars. *Geol. Soc. Finland Bull.* **40**, 59-64.
- LUTH, W.C., JAHNS, R.H. & TUTTLE, O.F. (1964): The granite system at pressures of 4 to 10 kilobars. *J. Geophys. Res.* **69**, 759-773.
- ____, MARTIN, R.F. & FENN, P.M. (1974): Peralkaline alkali feldspar solvi. In *The Feldspars* (W.S. MacKenzie & J. Zussman, eds.). Proc. NATO Adv. Study Inst. (Manchester 1972). Manchester Univ. Press, England.

- MANUYLOVA, M.M., PETROV, L.L., RYBAKOVA, M.M., SOKOLOV, YU.M. & SHMAKIN, B.M. (1966): Distribution of alkali-metals and beryllium in pegmatite minerals from the North Baikalian pegmatite belt. *Geochem.*, 309-321.
- MARTIN, R.F. (1974): Controls of ordering and subsolidus phase relations in the alkali feldspars. In *The Feldspars* (W.S. MacKenzie & J. Zussman, eds.). Proc. NATO Adv. Study Inst. (Manchester 1972). Manchester Univ. Press, England.
- (1982): Quartz and the feldspars. In *Granitic Pegmatites in Science and Industry* (P. Cerný, ed.). *Mineral. Assoc. Can., Short Course Handbook* 8, 41-62.
- & BONIN, B. (1976): Water and magma genesis: the association hypersolvus granite - subsolvus granite. *Can. Mineral.* 14, 228-237.
- MASON, R.A. (1982): Trace element distributions between the perthite phases of alkali feldspars from pegmatites. *Mineral. Mag.* 45, 101-106.
- , SMITH, J.V., DAWSON, J.B. & TREVES, S.B. (1982): A reconnaissance of trace elements in orthoclase megacrysts. *Mineral. Mag.* 46, 7-11.
- MORSE, S.A. (1970): Alkali feldspars with water at 5 kb pressure. *J. Petrology* 11, 221-253.
- NEIVA, A.M.R. (1977): Geochemistry of the pegmatites and their minerals from central northern Portugal. *Publ. Mus. Lab. Mineral. Geol. Fac. Cienc. Porto* 88, 1-32.
- NISSEN, H.-U. (1967): Domänengefüge, Natriumgehalt, Natriumentmischung und Gitterkonstanten von Alkalifeldspäten (Mikroclin, Orthoklas, Adular) des Schweizeralpen. *Schweiz. Mineral. Petrog. Mitt.* 47, 1140-1145.
- ORVILLE, P.M. (1960): Petrology of several pegmatites in the Keystone district, Black Hills, South Dakota. *Geol. Soc. Amer. Bull.* 71, 1467-1490.
- POVONDRA, P. & LANGER, K. (1971): Synthesis and some properties of sodium-beryllium-bearing cordierite, $\text{Na}_x\text{Mg}_2(\text{Al}_{4-x}\text{Be}_x\text{Si}_5\text{O}_{18})$. *Neues Jahrb. Mineral. Abh.* 116, 1-19.
- PRINCE, E., DONNAY, G. & MARTIN, R.F. (1973): Neutron diffraction refinement of an ordered orthoclase structure. *Amer. Mineral.* 58, 500-507.
- RINGWOOD, A.E. (1955): The principles governing trace element distribution during magmatic crystallization. *Geochim. Cosmochim. Acta* 7, 189-202, 242-254.
- SCHWARZER, T.F. (1969): *The Distribution of Major and Trace Elements in Co-existing Feldspar Pairs from Selected Pegmatites in New York State*. Ph.D. thesis, Rensselaer Polytechnic Institute, Troy, N.Y.
- SECK, H.A. (1972): The influence of pressure on the alkali feldspar solvus from peraluminous and per-silicic materials. *Fortschr. Mineral.* 49, 31-49.
- SHIMANSKII, A.A. & UCHAKIN, YU.M. (1962): Character of distribution of alkalis in the pegmatitic microclines of the Eastern Sayan Mountains. *Geochem.*, 957-961.
- SHMAKIN, B.M. (1979): Composition and structural state of K-feldspars from some U.S. pegmatites. *Amer. Mineral.* 64, 49-56.
- SIMPSON, D.R. (1977): Aluminum phosphate variants of feldspar. *Amer. Mineral.* 62, 351-355.
- SMITH, J.V. (1974): *Feldspar Minerals. 2. Chemical and Textural Properties*. Springer-Verlag, New York.
- SOLOMON, G.C. & ROSSMAN, G.R. (1979): The role of water in structural states of K-feldspar as studied by infrared spectroscopy. *Geol. Soc. Amer. Abstr. Programs* 11, 521.
- STEELE, I.M., HERVIG, R.L., HUTCHEON, I.D. & SMITH, J.V. (1981): Ion microprobe techniques and analyses of olivine and low-Ca pyroxene. *Amer. Mineral.* 66, 526-546.
- , HUTCHEON, I.D. & SMITH, J.V. (1980): Ion microprobe analysis of plagioclase feldspar for major, minor and trace elements. *Proc. 8th Int. Conf. on X-ray Optics and Micro-analysis (Boston)*, 515-525.
- STEWART, D.B. & ROSEBOOM, E.H. (1962): Lower temperature terminations of the three-phase region plagioclase - alkali feldspar - liquid. *J. Petrology* 3, 280-315.
- & WRIGHT, T.L. (1974): Al/Si order and symmetry of natural alkali feldspars, and the relationship of strained cell parameters to bulk composition. *Soc. franç. Minéral. Crist. Bull.* 97, 356-377.
- STRETENSKAYA, N.G. (1963): Conditions of formation of microcline in pegmatites in Kazakhstan. *Geochem.*, 691-697.
- STRUNZ, H., FORSTER, A. & TENNYSON, C. (1975): Die Pegmatite in der nördlichen Oberpfalz. A. Geologie und Genese. B. Mineralführung. *Aufschluss* 26, 117-189.
- TAN, L.-P. (1966): Major pegmatite deposits of New York State. *N. Y. State Mus. Sci. Service Bull.* 408.
- TAYLOR, B.E., FOORD, E.E. & FRIEDRICHSEN, H. (1979): Stable isotope and fluid inclusion studies of gem-bearing granitic pegmatite-aplite dikes, San Diego Co., California. *Contr. Mineral. Petrology* 68, 187-205.

- TAYLOR, S.R., HEIER, K.S. & SVERDRUP, T.L. (1960): Trace element variations in three generations of feldspars from the Landsverk I pegmatite, Evje, southern Norway. *Norsk Geol. Tidsskr.* **40**, 133-156.
- TUTTLE, O.F. & BOWEN, N.L. (1958): Origin of granite in the light of experimental studies in the system $\text{NaAlSi}_3\text{O}_8 - \text{KAlSi}_3\text{O}_8 - \text{SiO}_2 - \text{H}_2\text{O}$. *Geol. Soc. Amer. Mem.* **74**.
- VAUGHAN, D.E.W. (1963): *The Crystallization of the Spruce Pine and Harding Pegmatites*. M.Sc. thesis, The Pennsylvania State Univ., University Park, Pa.
- WRIGHT, T.L. & STEWART, D.B. (1968): X-ray and optical study of alkali feldspar. I. Determination of composition and structural state from refined unit-cell parameters and 2V. *Amer. Mineral.* **53**, 38-87.
- ZALASHKOVA, N.E. (1957): Albitization stages in granite pegmatites shown on an example of one of the pegmatite fields of Altai. *Trudy Inst. Mineral., Geochim. Kristallokhim. Redkikh Elementov*, 155-167 (in Russ.).
- Received August 9, 1983, revised manuscript accepted December 21, 1983.*